

RESEARCH ARTICLE

# Heat shock factor 2 regulates oncogenic gamma-herpesvirus gene expression by remodeling the chromatin at the ORF50 and BZLF1 promoter

Lorenza Cutrone<sup>1,2,3</sup>, Hedvig Djupenström<sup>1,2,3</sup>, Jasmin Peltonen<sup>1,2</sup>, Elena Martinez Klimova<sup>1,2,3</sup>, Simona Corso<sup>4,5</sup>, Silvia Giordano<sup>4,5</sup>, Lea Sistonen<sup>1,2</sup>, Silvia Gramolelli<sup>1,2,3\*</sup>

**1** Faculty of Science and Engineering, Cell Biology, Åbo Akademi University, Turku, Finland, **2** Turku Bioscience Centre, University of Turku and Åbo Akademi University, Turku, Finland, **3** InFLAMES Research Flagship Center, Åbo Akademi University, Turku, Finland, **4** Department of Oncology, University of Torino, Candiolo, Italy, **5** Candiolo Cancer Institute, FPO-IRCCS, Candiolo, Italy

\* [silvia.gramolelli@abo.fi](mailto:silvia.gramolelli@abo.fi)



**OPEN ACCESS**

**Citation:** Cutrone L, Djupenström H, Peltonen J, Martinez Klimova E, Corso S, Giordano S, et al. (2025) Heat shock factor 2 regulates oncogenic gamma-herpesvirus gene expression by remodeling the chromatin at the ORF50 and BZLF1 promoter. *PLoS Pathog* 21(4): e1013108. <https://doi.org/10.1371/journal.ppat.1013108>

**Editor:** John Karijovich, Vanderbilt University Medical Center, UNITED STATES OF AMERICA

**Received:** March 31, 2025

**Accepted:** April 7, 2025

**Published:** April 17, 2025

**Peer Review History:** PLOS recognizes the benefits of transparency in the peer review process; therefore, we enable the publication of all of the content of peer review and author responses alongside final, published articles. The editorial history of this article is available here: <https://doi.org/10.1371/journal.ppat.1013108>

**Copyright:** © 2025 Cutrone et al. This is an open access article distributed under the terms of the [Creative Commons Attribution License](https://creativecommons.org/licenses/by/4.0/),

## Abstract

The Human gamma-herpesviruses Kaposi's sarcoma herpesvirus (KSHV) and Epstein-Barr virus (EBV) are causally associated to a wide range of cancers. While the default infection program for these viruses is latent, sporadic lytic reactivation supports virus dissemination and oncogenesis. Despite its relevance, the repertoire of host factors governing the transition from latent to lytic phase is not yet complete, leaving much of this complex process unresolved. Here we show that heat shock factor 2 (HSF2), a transcription factor involved in regulation of stress responses and specific cell differentiation processes, promotes gamma-herpesvirus lytic gene expression. In lymphatic endothelial cells infected with KSHV and in gastric cancer cells positive for EBV, ectopic HSF2 enhances the expression of lytic genes; While knocking down HSF2 significantly decreases their expression. HSF2 overexpression is accompanied by decreased levels of repressive histone marks at the promoters of the lytic regulators KSHV ORF50 and EBV BZLF1, both characterized by poised chromatin features. Our results demonstrate that endogenous HSF2 binds to the promoters of KSHV ORF50 and EBV BZLF1 genes and shifts the bivalent chromatin state towards a more transcriptionally permissive state. We detected HSF2 binding to the ORF50 promoter in latent cells, in contrast, in lytic cells, HSF2 occupancy at the ORF50 promoter is lost in conjunction with its proteasomal degradation. These findings identify HSF2 as a regulator of gamma-herpesvirus lytic gene expression in latency and offer new insights on the function of this transcription factors at poised gene promoters, improving our understanding of its role in differentiation and development.

which permits unrestricted use, distribution, and reproduction in any medium, provided the original author and source are credited.

**Data availability statement:** All relevant data are within the manuscript and its [Supporting information](#) files

**Funding:** The study was supported by Finnish Society of Sciences and Letters, Mary and Georg Ehrnrooth Foundation and K. Albin Johansson Foundation, InFLAMES Research Flagship, South-west Finland Cancer Society to SGr; Sigrid Jusélius Foundation, Cancer Foundation Finland, The Medical Foundation Liv och Hälsa to L.S. LC, LS, SGr were supported by the Research Council of Finland; grant number 355708 (SGr, LC), 355596 (LS). SGr was also supported by the Finnish Cultural Foundation. SC and SGI were supported by the Italian association for Cancer research IG 27531 and by Italian Ministry of Health, Ricerca Corrente 2024-2025. The funders had no role in study design, data collection and analysis, decision to publish, or preparation of the manuscript.

**Competing interests:** The authors have declared that no competing interests exist.

## Author summary

The intricate interplay between cellular factors and viral gene regulation is crucial for understanding gamma herpesvirus biology and oncogenesis. A key aspect of their life cycle is the switch from the default latent state to the productive lytic replication, a process still not fully understood and increasingly involved in viral-induced oncogenesis. We identified heat shock factor 2 (HSF2) as a common positive regulator of gene expression in both human oncogenic gamma-herpesviruses: Kaposi's sarcoma-associated herpesvirus (KSHV) and Epstein-Barr virus (EBV). We demonstrated that HSF2 binds to the promoter of key lytic activators KSHV ORF50 and EBV BZLF1 during latency thereby modulating the local chromatin landscape. In the presence of HSF2 we observed a reduction in the repressive histone mark H3K27-me3, priming these promoters for reactivation and increasing the expression of the downstream lytic genes already in latency. Interestingly, during KSHV lytic cycle, HSF2 occupancy of the ORF50 promoter is lost and HSF2 is degraded by the proteasome. This work expands our knowledge of the complex transition from viral latency to lytic reactivation, highlighting the dynamic nature of host-virus interactions in diverse phases of the viral life cycle.

## Introduction

The gamma-herpesviruses Kaposi's sarcoma associated herpesvirus (KSHV) and Epstein-Barr virus (EBV) are human oncogenic herpesviruses, recognized by the World Health Organization (WHO) as class I carcinogens. Together they account for approximately 2–3% of all cancer cases worldwide ([www.globocan.com](http://www.globocan.com)). KSHV seroprevalence varies globally, with higher rates in regions like sub-Saharan Africa and the Mediterranean basin. KSHV is causally associated to primary effusion lymphoma, multicentric Castleman's disease and Kaposi's sarcoma (KS) [1,2]. EBV is a ubiquitous virus, infecting 95% of the human population and it was the first pathogen etiologically associated with human malignancies [3]. EBV infection is linked to various types of cancers, including endemic Burkitt's lymphoma, nasopharyngeal carcinoma (NPC), and EBV-associated gastric cancer (EBVaGC), a recently identified molecular subtype of gastric cancer [3–7].

While the default infection program for gamma-herpesviruses is latency, sporadic lytic reactivation episodes are essential for viral dissemination [8,9]. During latency, the viral genomes persist in the nucleus of the infected cells as circular episomes which are epigenetically silenced. The gene expression is restricted to a handful of latent genes that are fundamental for evading the immune surveillance and ensure host cell survival [10,11]. In contrast, during the lytic phase, all viral genes are expressed according to a well-orchestrated temporal cascade. The process initiates with the expression of early lytic genes that promote viral replication, followed by the late lytic genes needed for the assembly and release of infectious

viral progeny [8,9,12,13]. Clinical observations highlight the important contribution of lytic reactivation in tumorigenesis, as KS patients undergoing treatment with inhibitors of the lytic replication experience tumor regression [14]. Essential for initiation and completion the lytic cycle are the key transcription factors KSHV RTA and EBV RTA and Zebra 1, encoded by KSHV ORF50 and EBV BRLF1 and BZLF1, respectively [12]. A recent study demonstrated the diverse functions of EBV ZTA and RTA, the former is essential for lytic genome replication and the expression of lytic origin transcripts, whereas the latter is responsible for efficient expression of the early lytic viral genes. Expression of both EBV RTA and ZTA is essential for the late viral replication steps and completion of the lytic cycle. Although it is known that the expression of these viral factors induce the full lytic cascade, the molecular events governing their regulation remain still obscure [12,15].

Environmental stimuli, like hypoxia and oxidative stress, have been implicated in controlling the switch from latency to productive lytic replication of several herpesviruses [12,16]. These stressors stimulate, in turn, the expression of heat shock proteins (HSPs), including HSP70 and HSP90, which function as molecular chaperones and are often hijacked by the viral replication machineries [17,18]. HSPs are host factors required for productive viral replication, where large amounts of essential, structural viral proteins need to be appropriately folded [18]. Additionally, both HSP70 and HSP90 are associated with the newly produced EBV and KSHV viral particles [19]. HSP70 has been also shown to relocalize from the cytoplasm to the nucleus, where it forms dynamic structures adjacent to the viral replication and transcription compartments during KSHV lytic phase [20].

In response to stress, the inducible expression of genes encoding HSP70 and HSP90 is regulated by the specific members of the heat shock factor (HSF) family, *i.e.*, HSF1 and HSF2. HSF1 is the primary mediator of the acute stress responses, whereas HSF2 supports HSF1-mediated stress-related functions [21–23]. Upon acute stress, HSF1 undergoes extensive post-translational modifications, causing its release from the complex with HSPs, and forms either homotrimers or heterotrimers with HSF2 [24,25]. These HSF complexes drive the transcription of downstream genes by binding to specific *cis*-acting genomic motifs known as the heat shock elements (HSEs). Depending on the biological context, HSFs can function both together and independently from one another. In stress response, HSF1 and HSF2 share common targets, but different subsets of genes regulated exclusively by either HSF1 or HSF2 have also been identified [26,27]. In many solid tumors, HSF1 and HSF2 interact and together modulate subsets of genes fundamental for disease progression, whereas in breast cancer HSF2 alone has been shown to promote the abnormal proliferation of cancer cells [28,29]. In addition to regulating cellular stress responses and malignant progression, HSF2 has also been implicated in diverse cellular processes ranging from erythroid differentiation to spermatogenesis and corticogenesis [21,25,26,30–32].

In the context of herpesviral infections, recent studies have demonstrated that HSF1 activation is required for efficient replication of human herpesvirus 6A and human cytomegalovirus (HCMV) [33,34]. Furthermore, in EBV-infected cells, HSF1 is recruited to an HSE-enriched region within the promoter of the EBV latent gene EBNA-1, thereby promoting its expression [35]. In this study, we focus on HSF2, whose role in viral infection has remained unexplored. We provide evidence for HSF2 acting as a positive regulator of KSHV and EBV gene expression programs. We found that HSF2 regulates the KSHV ORF50 promoter independently from RTA and HSF1. Interestingly, endogenous HSF2 binds the ORF50 promoter in latent but not lytic cells and undergoes proteasomal degradation upon induction of KSHV lytic cycle. In the presence of ectopically expressed HSF2, the chromatin at the KSHV ORF50 promoter showed a decreased repressive chromatin mark, while HSF2 depletion increased this mark. Similarly, HSF2 positively regulates EBV gene expression and intracellular viral genome copies in EBVaGC organoids and EBV-infected gastric adenocarcinoma cell lines. Mechanistically, we detected endogenous HSF2 binding to the EBV BZLF1 promoter and decreased repressive chromatin marks in the context of HSF2 ectopic expression, indicative of a more permissive viral transcriptional state. This study expands our understanding of the multifaceted and dynamic interplay between oncogenic gamma-herpesviruses and the host cellular machinery.

## Results

### HSF2 expression modulates the lytic cycle in KSHV-infected lymphatic endothelial cells

To investigate the potential role of HSF2 in KSHV life cycle, we perturbed its expression in lymphatic endothelial cells infected with the rKSHV.219 strain (indicated here as KLEC). KLEC support a spontaneous KSHV lytic expression program. In these cells, lytic expression as well as infectious progeny production and release occur without any trigger. We decided to use this cell model as KLEC are putative cells of origin of KS, thus representing a relevant *in vitro* model for studying the regulatory mechanisms of KSHV gene expression and tumorigenesis [8,36–38].

First, we overexpressed either HSF2 or a GFP control vector by lentiviral transduction in KLEC for 72 h and demonstrated elevated HSF2 protein levels by immunoblot (Fig 1A). We observed a pronounced increase in KSHV early (K-bZIP) and late (K8.1) lytic protein expression (Fig 1A) along with a concomitant elevated expression of lytic genes, including *ORF57* and *ORF50* (Fig 1B). HSF2 overexpression also enhanced secretion of viral particles from the infected cells (Fig 1C). Subsequently, we tested the effect of HSF2 downregulation on KSHV expression and virus release. KLEC were transiently transfected with either a control (scr) siRNA or an siRNA targeting HSF2 for 72 h. Efficient silencing of HSF2 and consequent protein downregulation was demonstrated by immunoblot (Fig 1D). A significant reduction in KSHV lytic protein levels and gene expression was observed (Fig 1D and 1E), along with diminished virus titers (Fig 1F).

Another cellular model where KSHV displays spontaneous lytic reactivation in a subpopulation of cells is the HEK293 [39]. To test the effect of HSF2 on viral gene expression, we first generated HEK293FT cells stably infected with rKSHV.219 (indicated as HEK.219) and subsequently silenced HSF2 by transient siRNA transfection. Compared to control treated cells, we observed a significant reduction in viral gene and protein expression in the cells treated with siRNA targeting HSF2, indicating that HSF2 regulates KSHV gene expression also in this cell type (S1A and S1B Fig).

These findings show that perturbing HSF2 levels influences KSHV gene expression, thereby pointing to HSF2 as a novel positive regulator of KSHV gene expression and viral production in primary KLEC and in HEK.219.

### HSF2 regulates the KSHV lytic gene expression during latent and lytic phases

To determine whether HSF2 modulates KSHV gene expression during latency or at the onset of the lytic phase, we opted for the iSLK.219 cells, a different cell-based system. Although representing a physiologically relevant model of KSHV infection, KLEC feature a continuous and asynchronous lytic reactivation. Therefore, the cellular events occurring in latency cannot be distinguished from those characterizing the lytic replication. Instead, iSLK.219 cells sustain a latent infection program with only a minute fraction (less than 1%) of cells undergoing spontaneous lytic reactivation [39]. These cells have been engineered to harbor an ectopic, doxycycline inducible *ORF50* gene for the expression of viral RTA, necessary and sufficient to induce the lytic cycle. In addition, iSLK.219 cells are infected with a recombinant rKSHV.219 virus which harbors a constitutively expressed GFP gene and an RFP reporter expressed only during lytic cycle, controlled by the early viral lytic polyadenylated nuclear RNA (PAN) promoter [39,40]. Thus, iSLK.219 cells represent an optimal model for accurate monitoring of the lytic reactivation which can be efficiently induced by doxycycline treatment.

We used lentiviral transduction to express either HSF2 or a GFP control in latent iSLK.219 cells for 48 h followed by a 24-h treatment with doxycycline. Immunoblot analysis showed higher levels of HSF2 upon overexpression and a concomitant increase in early and late lytic viral proteins, K-bZIP and K8.1, respectively (Fig 2A). Moreover, we observed a statistically significant higher number of RFP-positive cells (Fig 2B). The augmented lytic reactivation was also measured at the transcriptional level, with significantly higher *ORF57* (early lytic) and *K8.1* gene expression in cells with ectopic HSF2 (Fig 2C). To validate our results, we investigated the effect of transient HSF2 depletion during the lytic phase in iSLK.219 cells. To this aim, we used siRNA targeting HSF2 or a control siRNA (siscr) for transfecting iSLK.219 cells and 48 h later we induced the lytic cycle by doxycycline treatment for 24 h. Immunoblot analysis showed a robust HSF2 downregulation and

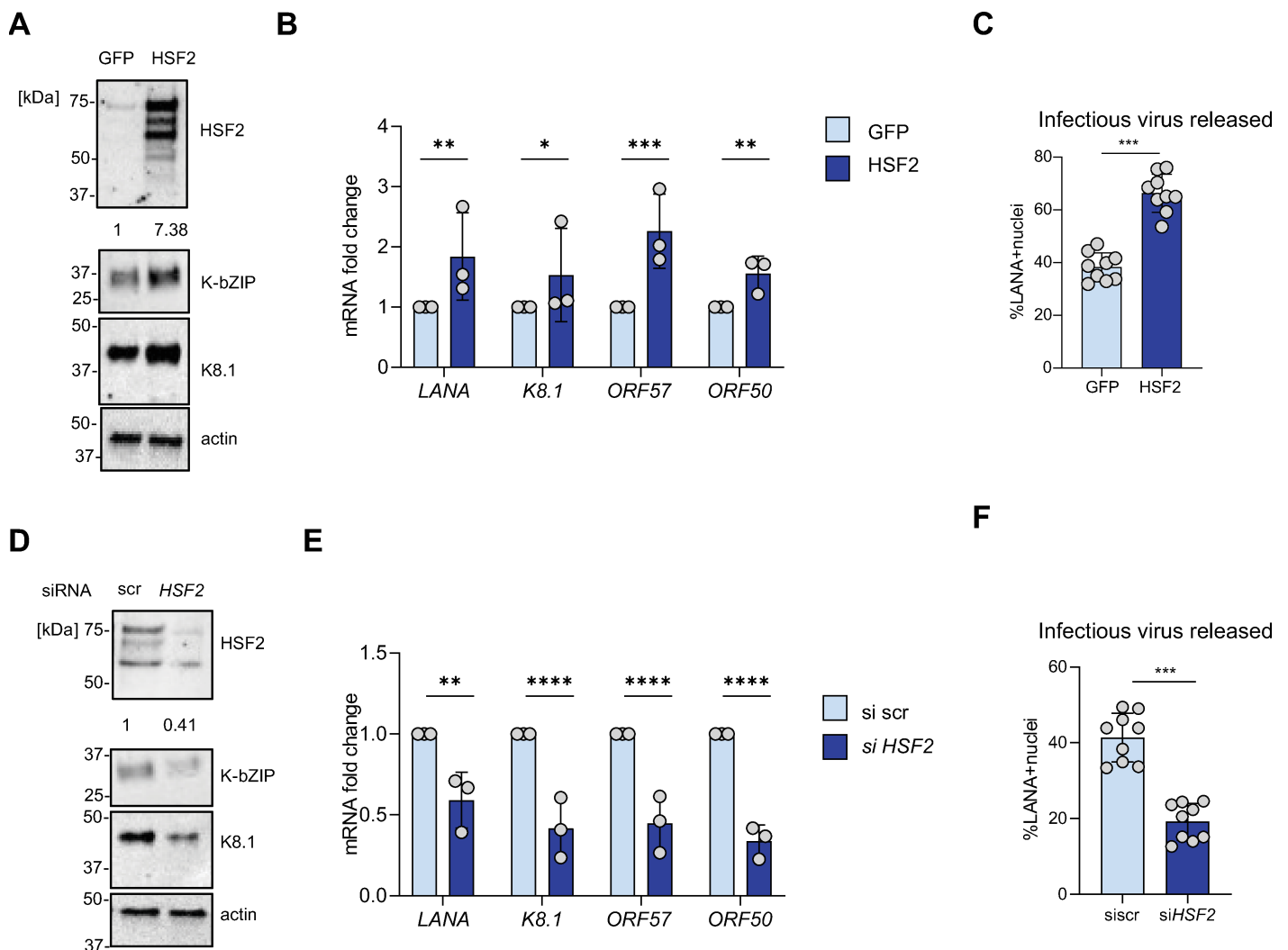


**Fig 1. HSF2 expression sustains KSHV infection in KLEC.** Primary LEC were infected with KSHV for 14 days. (A, B, C) KLEC were transduced with lentiviruses carrying either a GFP or a HSF2 gene for 72h prior to analysis. (D, E, F) KLEC were treated with siRNA control (scramble, scr) or targeting HSF2 for 72h prior to analysis. (A, D) Representative Immunoblot analysis of HSF2 and viral K-bZIP and K8.1 proteins, actin was used as a loading control. Molecular weight in kDa is shown on the left. Numbers below the HSF2 blot indicate the relative band intensities normalized to the appropriate loading control. (B, E) RTqPCR analysis of the indicated transcripts. *Actin* was used as an internal control. Transcript fold changes relative to GFP (B) sisr (E) are shown. Bars indicated average, error bars the standard deviation across three independent experiments, single data points are indicated as grey circles (C, F) the supernatant from KLEC treated as indicated was serially diluted and applied to uninfected U2OS cells for 24h. Cells were stained for LANA, nuclei were counterstained with DAPI and imaged with high throughput microscope. Percentage of LANA positive nuclei are shown. Bars indicated average, error bars the standard deviation across independent experiments, single data points are indicated as grey circles.

<https://doi.org/10.1371/journal.ppat.1013108.g001>

lower levels of the K-bZIP viral protein (Fig 2D). Additionally, HSF2 depletion led to a significant decrease in RFP-positive cells (Fig 2E) and in viral gene expression (Fig 2F).

Since the effect of HSF2 modulation on KSHV expression was evident already at 24h after doxycycline induction, we asked whether HSF2 would influence the levels of lytic viral gene expression prior to the induction of the lytic cycle, *i.e.*, in latently infected cells. To answer this question, we measured viral gene expression in latent iSLK.219 cells overexpressing HSF2 for 48h and observed significantly increased expression of LANA, ORF57 and K8.1 (Fig 2G). Similarly, also endogenous ORF50 transcript levels were significantly upregulated in latent iSLK.219 cells overexpressing HSF2 (Fig 2G). The

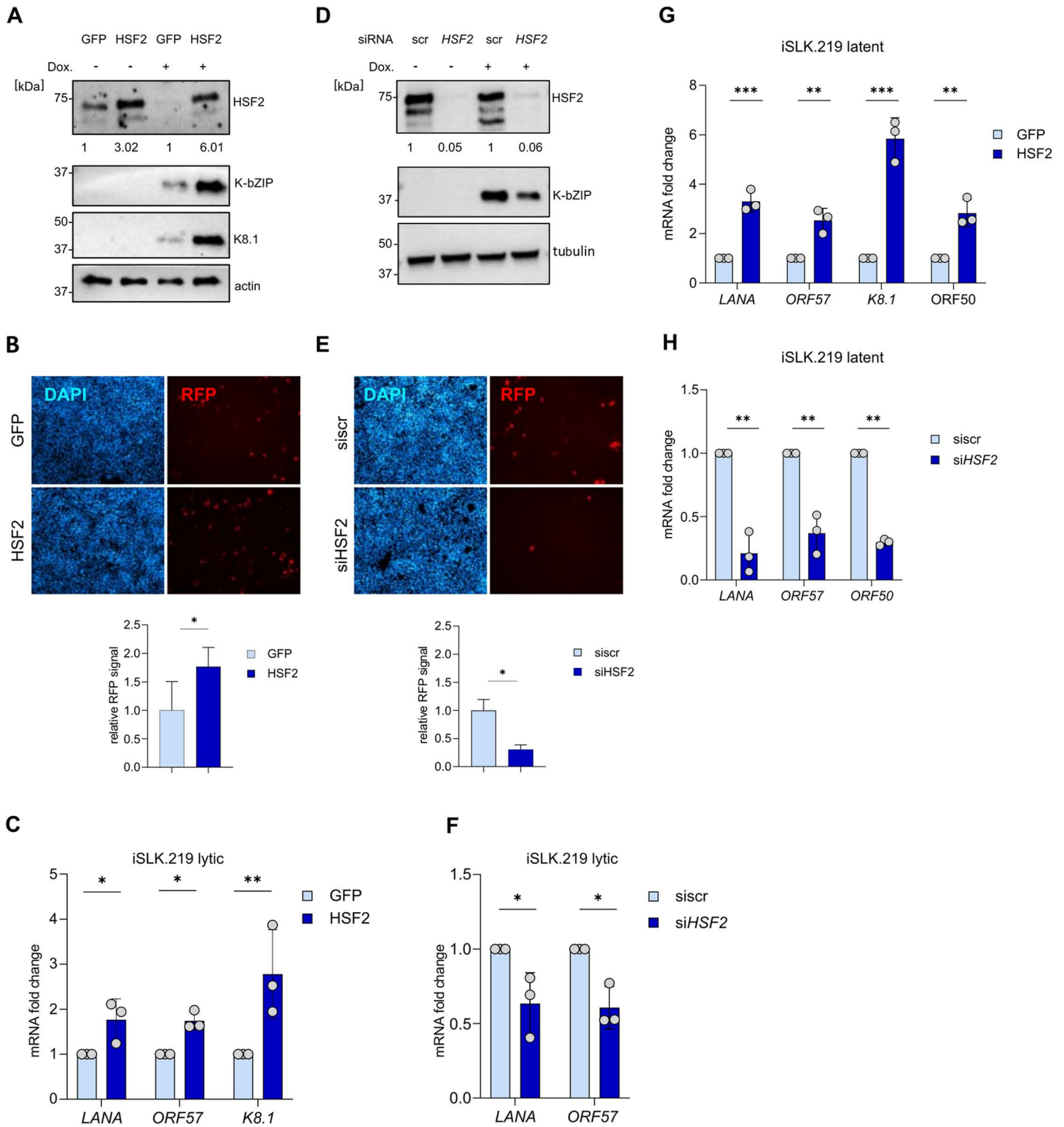


**Fig 2. HSF2 regulates lytic gene expression in latency and during the lytic phase.** (A) iSLK.219 cells were transduced with GFP or HSF2 encoding lentiviruses for 48 h, where indicated Doxycycline (DOX) treatment was added for 24 h. Cell lysate was analyzed by immunoblot for HSF2 and for the viral proteins K-bZIP and K8.1. Actin was used as a loading control. Representative blots are shown. Molecular weight in kDa is shown on the left.

Numbers below the HSF2 blot indicate the relative band intensities normalized to the appropriate loading control. **(B)** Fluorescent microscopy images of iSLK.219 cells treated as in (A) and reactivated with Doxycycline for 24 h and stained with DAPI. Scale bar 100  $\mu$ m. **(C)** iSLK.219 cells were treated as in (A) and analyzed by RTqPCR for the indicated viral transcripts. Transcript fold changes relative to GFP are shown. *Actin* was used as an internal control. Bars indicate the average and the error bar the SD across three independent experiments, single data points are shown as grey circles. **(D)** Representative immunoblot analysis of iSLK.219 cells transfected with the indicated siRNAs for 48 h, where indicated Doxycycline (Dox) treatment was added for 24 h. Cell lysate was analyzed by immunoblot for HSF2 and for the viral protein K-bZIP. *Tubulin* was used as a loading control. Molecular weight in kDa is shown on the left. Numbers below the HSF2 blot indicate the relative band intensities normalized to the appropriate loading control. **(E)** Fluorescent microscopy images of iSLK.219 cells treated as in (D) and reactivated with Doxycycline for 24 h and stained with DAPI. Scale bar 100  $\mu$ m. **(F)** iSLK.219 cells were treated as in (E) and analyzed by RTqPCR for the indicated viral transcripts. Transcript fold changes relative to *siscr* are shown *Actin* was used as an internal control. Bars indicate the average and the error bar the SD across three independent experiments, single data points are shown as grey circles. **(G, H)** iSLK.219 cells were transfected with the indicated lentiviruses for 48 h **(G)** or transfected with the indicated siRNA **(H)**. Transcript fold changes relative to GFP are shown. *Actin* was used as an internal control. Bars indicate the average and the error bar the SD across three independent experiments, single data points are shown as grey circles.

<https://doi.org/10.1371/journal.ppat.1013108.g002>

endogenous ORF50 transcripts were detected with forward primer binding the 5'UTR sequence which is absent in the ectopic, doxycycline inducible ORF50 gene (Fig 2G). Conversely, silencing HSF2 in latent iSLK.219 cells led to significantly reduced levels of viral transcripts (Fig 2H). Together, these results reveal that HSF2 enhances KSHV gene expression in both lytically reactivated iSLK.219 cells and during latency.

### Ectopic HSF2 regulates the KSHV ORF50 promoter independently of RTA and HSF1

The effect of HSF2 on the KSHV gene expression was demonstrated at the transcriptional level. Therefore, we reasoned that HSF2 could enhance KSHV gene expression by regulating viral promoter activities. We investigated this hypothesis by performing luciferase reporter assays in cells expressing ectopic HSF2. We selected a set of plasmids harboring the reporter gene downstream of individual viral promoters which were co-transfected with either HSF2 or GFP control expressing vectors. Efficient HSF2 overexpression was demonstrated by immunoblot (S2A–D Fig). In these experiments, we did not observe any significant variation in the activity K8.1 or ORF45 lytic promoters in the presence of ectopic HSF2 (Fig 3A). Similarly, ectopic HSF2 had no significant impact on the activity of either the 7XTR promoter, containing seven copies of KSHV latent origin of viral replication, or on the KSHV origin of lytic replication, ORILYT (Fig 3B). However, we detected a strong increase in the activity of the ORF50 promoter in conjunction with HSF2 overexpression (Fig 3C).

ORF50 codes for RTA, the master transcriptional regulator of the KSHV lytic cycle. Beside other downstream lytic promoters, RTA also binds to and increases the activity of its own promoter in a positive feedback loop [41]. This is fundamental to enhance the efficiency of the lytic reactivation thus ensuring its progression and successful completion [15,41,42]. Several cellular transcription factors have been implicated in assisting RTA to further reinforce this positive feedback loop. Examples include cellular PROX1, which is expressed in lymphatic endothelial cells and functions as a key contributor to the spontaneously lytic KSHV expression program observed in the lymphatic cellular environment [38]. To test whether HSF2 would synergize with RTA, we co-expressed both proteins together with the luciferase ORF50 reporter. KSHV RTA significantly increased the activity of the ORF50 promoter, in line with previously published results [43]. However, the presence of HSF2 did not potentiate this effect (Fig 3D). From these results we concluded that HSF2 regulates the expression of ORF50 by increasing its promoter activity in the absence of RTA protein expression.

HSF2 is a transcription factor that can act either directly on its target genes or together with HSF1 [21,27]. During acute stress the interplay between HSFs sustains an optimal cellular response, whereas in other physiological and pathological processes such as erythroid differentiation and breast cancer progression, HSF2 operates independently from HSF1 [21,29,31]. To address whether HSF2 would act in concert with HSF1 in regulating the KSHV life cycle, we transiently silenced HSF1 for 48 h in latent iSLK.219 cells expressing either ectopic HSF2 or GFP control. Immunoblot analysis showed that upon robust silencing of HSF1, HSF2 levels were also diminished (Fig 3E), which is in line with previous reports documenting lower HSF2 levels in cells devoid of HSF1 [22,24,44]. In contrast, when ectopically reintroduced,

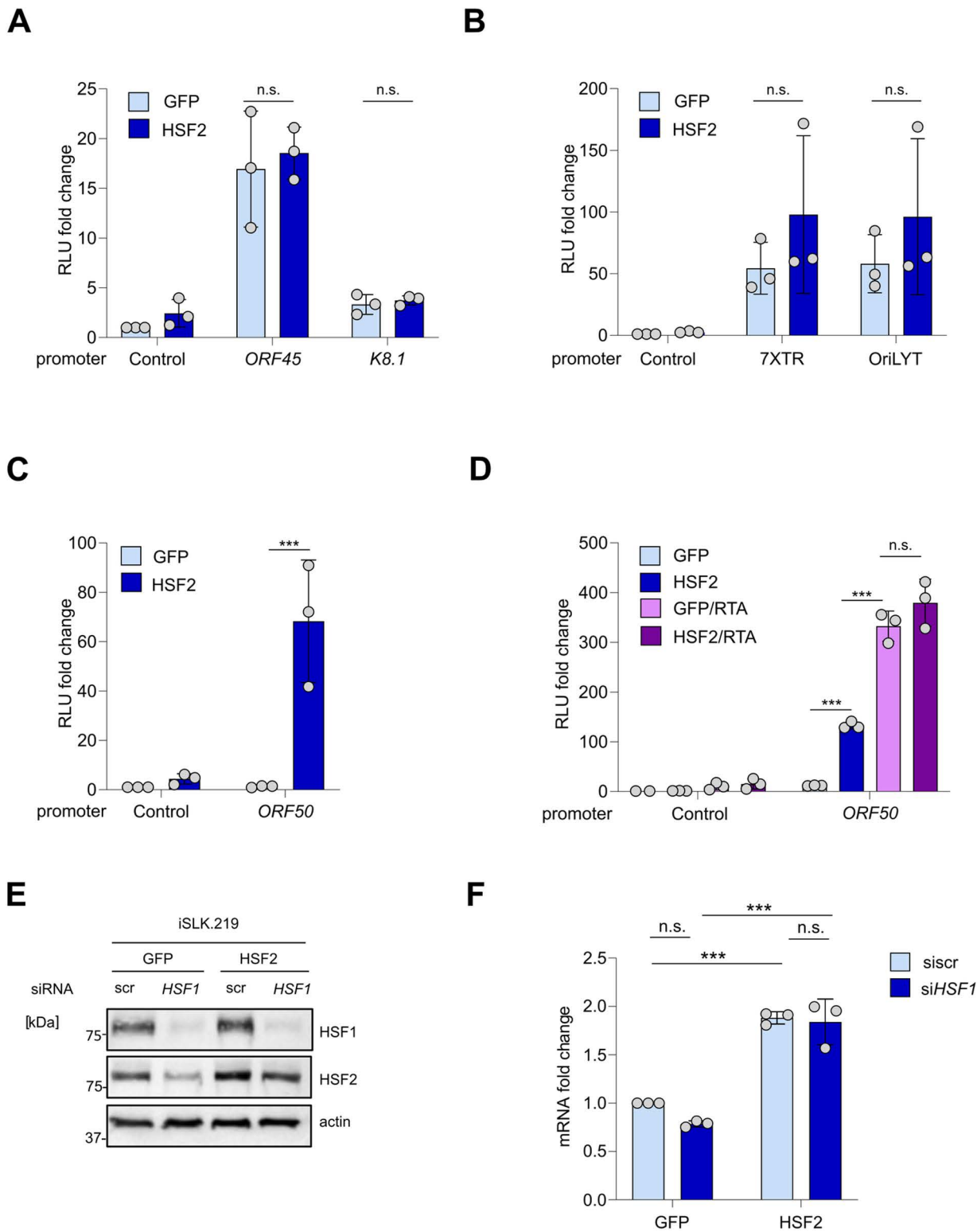


**Fig 3. HSF2 regulates ORF50 expression in an RTA independent manner.** (A–D) Luciferase reporter assay in HEK293FT cells co transfected in triplicate with a plasmid harboring the luciferase reporter gene downstream of a control basic promoter (control) or the indicated viral promoters (A, C, D) or viral origins of replication (B), along with HSF2 or GFP control expressing plasmids. In (D) cells were also transfected with an RTA-encoding plasmid.

Luciferase activity was measured 48h after transfection and indicated as relative luciferase units (RLU) fold change compared to the control -GFP sample. The experiments were repeated three independent times, each datapoint (grey circle) represents the average of the three technical replicates, bars represent the average across three biological replicates, and the error bars the SD across three independent biological replicates. **(E)** Representative immunoblot analysis for HSF1 and HSF2 in iSLK.219 cells overexpressing GFP or HSF2 and transfected with either control (scr) siRNA or siRNA targeting HSF1 for 48 hours. *Actin* was used as loading control. Molecular weight in kDa is shown on the left. **(F)** RTqPCR analysis of cells treated as in (E) for *ORF50* gene, *Actin* was used as loading control. Transcript fold changes relative to GFP, scr-treated sample are shown. *Actin* was used as an internal control. Bars indicate the average and the error bar the SD across three independent experiments, single data points are shown as grey circles.

<https://doi.org/10.1371/journal.ppat.1013108.g003>

HSF2 levels were not as dramatically affected by HSF1 depletion. In these cells, ORF50 expression was upregulated upon HSF2 overexpression even when HSF1 was depleted (Fig 3F). In U2OS osteosarcoma cells stably infected with KSHV, where a less robust HSF1 depletion was obtained, we confirmed that HSF2 overexpression increased ORF50 levels regardless of HSF1 silencing (S2E and S2F Fig).

These results reveal that in the context of the KSHV life cycle, ectopic HSF2 enhances the activity of the ORF50 promoter independently of both RTA and HSF1. The ability of HSF2 to affect ORF50 expression in the absence of RTA supports our observation that HSF2 can modulate lytic genes already in latent cells. Importantly, we also show that during latent KSHV infection HSF2 levels are controlled by HSF1, similarly to what has been shown for uninfected cells. Furthermore, our results demonstrated that overexpressed HSF2 is capable of regulating ORF50 expression in an HSF1-independent manner. This underscores a separate mechanism that diverges from the previously reported roles of HSF1 in controlling other herpesviral life cycles and gene expression [33–35].

### HSF2 binds the ORF50 promoter and modifies the local epigenetic landscape

*In vitro* and *in vivo* studies have demonstrated that HSF2 protein recognizes classic heat shock elements (HSEs) on the promoter of its target genes [31,45,46]. The HSEs contains a variable number of the pentameric sequence nGAAn arranged in alternate orientation [47]. We used the JASPAR database to screen the ORF50 promoter for the presence of this motif. We identified a putative HSE displaying a stretch of three nGAAn pentamers located in the region from 546 to 559 nucleotides upstream of the ORF50 transcriptional start site (TSS) (the position of the HSE motif within the ORF50 promoter is highlighted in yellow on the schematics in Fig 4A, and its nucleotide sequence is shown below along with the HSE sequence logo). To experimentally test the possible binding of HSF2 to the ORF50 promoter, we performed a chromatin immunoprecipitation assay followed by RTqPCR (ChIP-PCR). We used a polyclonal HSF2 antibody [22] to precipitate endogenous HSF2 and amplified a region covering about 800 base pairs (bp) upstream of the ORF50 TSS (Fig 4A). Endogenous HSF2 occupied the ORF50 promoter in latent cells (Fig 4B). To our surprise, in iSLK.219 cells reactivated for 24 h, no HSF2 binding was detected at the ORF50 promoter (Fig 4C), indicating a possible displacement of HSF2 during the lytic replication cycle. To address whether endogenous HSF2 was recruited to the chromatin during the early stages of lytic reactivation, we tested the cellular HSP70 promoter, a known HSF2 target [22] (Fig 4D). We observed HSF2 binding on the HSP70 promoter in both latent and lytic (treated with Dox for 24 hours) cells, indicating that HSF2 is still capable of occupying the chromatin. As an additional control, we tested other regions of the KSHV genome, one localized in proximity of the ORF73 gene, coding for the key latent protein LANA and the other localized within the late lytic K8.1 promoter. In these regions, we did not detect any HSF2 binding either in latent or in lytic cells (S3A and S3B Fig).

Epigenetic profiling of the KSHV genome has revealed that, during latency, the KSHV ORF50 promoter bears concomitant activating and repressive histone marks in its chromatin structure characterized by the deposition of tri-methyl groups on either lysine 4 or 27 of the histone H3 (H3K4-me3 and H3K27-me3, respectively) [48]. This bivalent or poised state is commonly found in pluripotent stem cells, at the promoters of genes regulating development [49]. Under unstimulated conditions, poised gene promoters remain transcriptionally repressed. However, upon receiving appropriate stimuli and concurrent removal of repressive marks, these promoters can rapidly become active thereby leading to gene expression [49,50]. Similarly, in the latent phase, the KSHV ORF50 promoter, which bears chromatin markers indicative of a

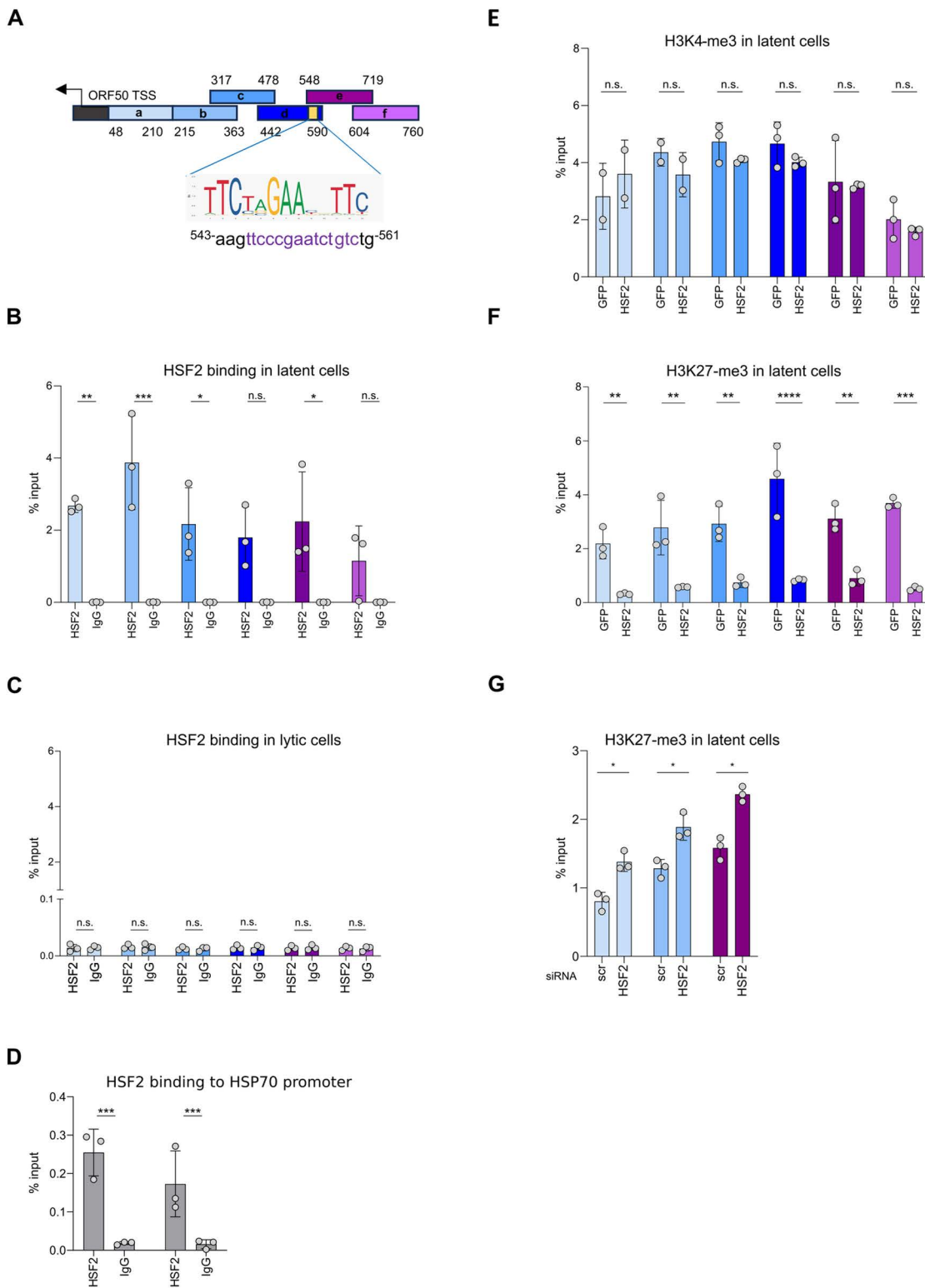


**Fig 4. HSF2 binds the ORF50 promoter and remodels the local chromatin landscape.** (A) Schematics of the ORF50 promoter region, transcription start site (TSS, black arrow) and HSF2 binding site (yellow box) are shown. The different genomic regions amplified by RTqPCR are depicted as blue and purple segments, the nucleotide positions relative to the TSS are labeled. The DNA motif and the nucleotide sequence identified as HSF2

consensus sequence, along with the HSE sequence logo are shown below. **(B, C)** ChIP-qPCR analysis of endogenous HSF2 binding to the ORF50 promoter regions expressed as % of input in KSHV infected latent **(B)** and reactivated with doxycycline for 24 h **(C)**. **(D)** ChIP-qPCR analysis of endogenous HSF2 binding to the cellular HSP70 promoter regions expressed as % of input in KSHV infected latent (left bars) and reactivated (right bars) with doxycycline for 24 h **(E, F)** ChIP PCR analysis of the indicated histone H3 modifications in latent iSLK.219 cells overexpressing HSF2 or GFP. The bars are colored according to the schematic in **(A)**. **(G)** ChIP PCR analysis of H3K27-me3 in latent iSLK.219 cells treated with the indicated siRNAs. Bars are colored according to the schematics in **(A)**. Bars represent the average and error bars the SD across three independent experiments, data points are indicated as grey circles.

<https://doi.org/10.1371/journal.ppat.1013108.g004>

poised state, remains silenced. Upon activation of the lytic cycle, the ORF50 promoter undergoes rapid activation with the removal of the repressive H3K27-me3 chromatin mark [11,48]. We then asked whether HSF2 would affect the bivalent chromatin state of the ORF50 promoter. For this, we performed a ChIP-PCR analysis in latently infected iSLK.219 cells transduced with either HSF2 or GFP control lentivirus. We used antibodies against H3K4-me3 and H3K27-me3, epigenetic marks for active and repressive chromatin, respectively. While the levels of activating H3K4-me3 were unchanged upon HSF2 overexpression across the ORF50 promoter (Fig 4E), the H3K27-me3 repressive chromatin mark was significantly diminished (Fig 4F). As control, we tested the levels of H3K4-me3 and H3K27-me3 in the KSHV genomic regions where HSF2 was not binding, and no change in the chromatin status was detected in cells overexpressing HSF2 (S3C and S3D Fig). Immunoblot is a common approach for assessing the global changes on specific histone modifications [51–53] and we used this technique to detect global variation in the levels of H3me3K27 levels in iSLK.219 cells overexpressing either HSF2 or GFP control. We found no detectable changes (S3E Fig), indicating that the variations in H3K27-me3 marks are localized to specific viral genomic loci rather than being broadly distributed. To extend our analysis we also tested by ChIP-PCR the levels of H3K27-me3 in latent iSLK.219 depleted of HSF2 by transient siRNA transfection (Fig 4G). Depletion of HSF2 led to significantly higher H3K27-me3 repressive chromatin marks on the ORF50 promoter, confirming our observations in the context of HSF2 overexpression.

These results indicate that HSF2 associates with the ORF50 promoter iSLK.219 cells during latency but not in the lytic phase. In latent cells HSF2 overexpression shifts the bivalent chromatin state of the ORF50 promoter by reducing locally H3K27-me3 levels, whereas silencing HSF2 is accompanied by an increment in this chromatin mark. Therefore, during KSHV latency, HSF2 primes the viral genome to transition from latency to lytic reactivation.

### HSF2 protein is degraded during the lytic reactivation

The remarkable loss of HSF2 occupancy to the ORF50 promoter 24 h after induction of the lytic cycle prompted us to investigate whether this was due to downregulation of HSF2 levels or to mislocalization of this transcription factor. To address these hypotheses, we performed both immunofluorescence staining and immunoblotting in iSLK.219 cells that were either latent or reactivated. Immunofluorescence revealed a nuclear localization of HSF2 in both latent and lytic (Dox. 24 h) cells. We measured a significant reduction of HSF2 intensity in the lytic cell population, compared to the latently infected cells (Fig 5A and 5B). As control we tested the levels of H3K4-me3 in latent and lytic cells and found no significant changes in signal intensity (S4A and S4B Fig). We next monitored HSF2 levels by immunoblot in iSLK.219 during a 48-h time-course following lytic reactivation (Fig 5C). We observed no changes 6 h after the induction of the lytic cycle followed by a gradual decrease at later timepoints. Together, these results suggest that HSF2 protein is downregulated rather than mislocalized during the KSHV lytic cycle.

During the lytic reactivation, cellular transcripts are degraded as a result of a process called viral-mediated host shut-off [54,55]. Earlier studies have estimated that approximately 80% of host transcripts undergo fast turnover due to KSHV-mediated host shut-off [54,56]. The viral exonuclease coded by the ORF37 gene and expressed during KSHV lytic phase is responsible for this process [55]. The host shut-off is necessary to ensure immune evasion and the preferential usage of the cellular translation machinery to produce viral proteins. Only a minor group of cellular transcripts escape the host shut-off, but the full list of escapees and the mechanisms behind this phenomenon are still incomplete [56,57]. We reasoned

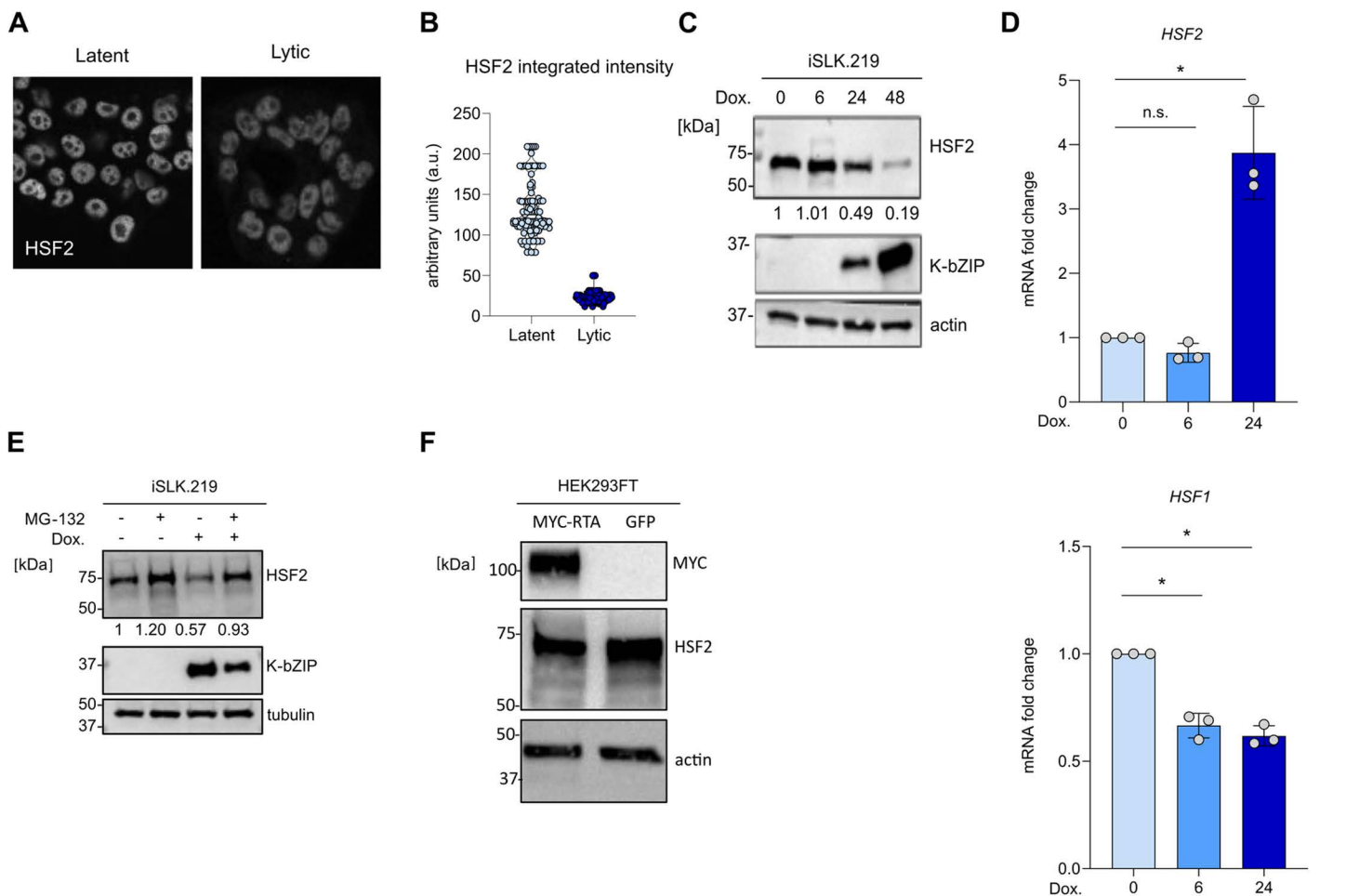


**Fig 5. HSF2 is degraded during KSHV lytic reactivation.** (A) Confocal representative images and (B) quantification of the HSF2 nuclear integrated HSF2 intensity in  $n > 100$  cells in iSLK.219 either latent or induced to the lytic cycle with doxycycline for 24h (indicated as lytic) and stained with an antibody against HSF2. (C) Representatives immunoblot analysis of iSLK.219 cells treated with doxycycline (Dox) for the indicated hours. Levels of HSF2 are shown, K-bZIP and actin are used as reactivation marker and loading control, respectively. Molecular weight in kDa is shown on the left. Numbers below the HSF2 blot indicate the relative band intensities normalized to the appropriate loading control. (D) Transcript analysis of *HSF2*, *HSF1* genes in iSLK.219 cells reactivated with doxycycline (Dox) for the indicated hours. *Actin* was used as internal control. Bars represent the average and error bars the SD across three independent experiments, data points are indicated as grey circles. (E) Representatives immunoblot analysis of iSLK.219 cells latent or induced with Doxycycline for 22h and were indicated treated with the MG132 proteasome inhibitor (+) or DMSO solvent control (-) for 3h prior to lysis. HSF2 protein levels are shown, K-bZIP and *tubulin* were used as lytic marker and loading control respectively. Molecular weight in kDa is shown on the left. Numbers below the HSF2 blot indicate the relative band intensities normalized to the appropriate loading control. (F) Immunoblot analysis of HEK293FT cells transfected for 24h with either myc-tagged RTA or a GFP control. Actin was used as loading control. Molecular weight in kDa is shown on the left.

<https://doi.org/10.1371/journal.ppat.1013108.g005>

that the reduction of HSF2 protein levels documented in lytic cells could result from the increased transcript turnover due to the ongoing host shut-off. To verify this result, we measured HSF2 mRNA levels over a 24-h time-course in iSLK.219 cells induced into the lytic cycle by doxycycline treatment and ORF57 transcript levels were also monitored to control the lytic reactivation efficiency (S4C Fig). To our surprise, no reduction in the levels of the HSF2 mRNA was detected (Fig 5D). When measuring HSF2 transcript levels, we found a significant increase in expression 24h following lytic reactivation, whereas HSF1 levels were downregulated during the analyzed time-course. This result indicated that HSF2 (but not HSF1) may belong to the small group of host transcripts that escape KSHV-induced host shut-off.

Since diminished HSF2 protein levels were not due to a reduced transcript turnover, we decided to investigate whether HSF2 downregulation was the result of proteasomal degradation. Interestingly, previous studies have shown that the levels of HSF2 protein can be regulated through the ubiquitin-proteasome pathway. For example during acute stress responses as well as in mitotically arrested cells, HSF2 is ubiquitinated and degraded by the proteasome, in a process mediated by the ubiquitin E3 ligase anaphase promoter complex APC/C [58,59]. To investigate whether HSF2 was subjected to proteasomal degradation during KSHV lytic phase, we treated iSLK.219 cells with the proteasome inhibitor MG132 for 3 h in both latent and lytic phase (treated with doxycycline for 24 h) and measured the levels of HSF2 by immunoblot. Results show that in lytic cells the inhibition of the proteasome activity rescued the levels of HSF2, hence implying that during the lytic replication cycle HSF2 protein levels are diminished because of proteasomal degradation (Fig 5E). The gene product encoded by ORF50, RTA, is not only a key activator of viral gene expression but also exhibits E3-ubiquitin ligase activity, targeting specific proteins for proteasomal degradation [60]. While the complete list of RTA targets remains unknown, some cellular proteins including RUNX3, and HEY1 have been identified as targets for ORF50-mediated degradation [61,62]. Based on the kinetics of HSF2 protein degradation and the rescue of this phenomenon by proteasome inhibitor treatment, we investigated whether ectopic RTA expression outside of KSHV infection cycle could induce HSF2 downregulation. Uninfected HEK293FT cells were transiently transfected with plasmids encoding either GFP (control) or myc-tagged RTA, and HSF2 levels were assessed by immunoblot. Our results showed decreased HSF2 levels in the presence of ectopic myc-RTA, suggesting that RTA plays a role in the downregulation of HSF2 during the KSHV lytic cycle (Fig 5F).

These results indicate that HSF2 is subjected to multiple regulatory modalities during lytic KSHV infection: While HSF2 transcript levels are significantly higher possibly due to increased transcription and/or host shut-off escape, the HSF2 protein levels are diminished because of proteasomal degradation. Additionally, RTA expression negatively impacts HSF2 levels also in uninfected cells, suggesting its involvement in HSF2 downregulation.

### HSF2 supports EBV gene expression

Several cellular factors modulate the reactivation of both gamma herpesviruses, EBV and KSHV, underscoring the existence of conserved mechanisms of regulation. Examples include, but are not restricted to, the Barrier-to-autointegration factor 1 (BAF1), Polo-like kinase 1 (PLK1) Aurora Kinase and the mitochondrial protein TBRG4 [63–65]. Based on our findings uncovering the positive role of HSF2 in KSHV reactivation, we asked whether EBV would also be subjected to a similar regulatory mechanism. It has been demonstrated that EBV displays a spontaneous lytic cycle in epithelial cells [66–68]. Due to its recently discovered role as causal agent of a molecular subtype of gastric cancer [7], we decided to test the effect of HSF2 in EBV life cycle using EBV-associated gastric cancer primary cells obtained from patient-derived xenografts (PDXs). These cells have been derived from EBVaGC patients, transplanted as xenografts in mice before culturing them *in vitro* [69]. We treated these cells with siRNA targeting HSF2 or a control, scr siRNA for 72 h and assessed EBV viral gene expression by RTqPCR. All analyzed viral genes were downregulated including latent (*EBNA1*), the early lytic (*BZRLF1* and *BRLF1*), and the late lytic (*BDLF1*) (Fig 6A).

For subsequent analysis, we decided to utilize the AGS model, a gastric adenocarcinoma cell line, ectopically infected with EBV akata strain (AGS BX1) [70]. We genetically deleted HSF2 using CRISPR Cas9 and established a stable AGS BX1 HSF2KO cell line (here indicated as 2KO cells). Lower HSF2 levels were confirmed by immunoblot and we observed a significant downregulation of EBV viral gene expression and reduced levels of the lytic protein Zebra 1 (Fig 6B and 6C). Genetic deletion of HSF2 was also accompanied by diminished intracellular viral genome copies (Fig 6D). To further validate our findings, we assessed the effect of HSF2 overexpression, and utilized AGS BX1 to generate stable cell lines ectopically expressing either HSF2 or a GFP control lentivirus. In these cells, EBV viral gene expression was significantly higher in HSF2-overexpressing cells when compared to the GFP control (Fig 6E). Conversely, also the level of the lytic protein Zebra 1 and the intracellular EBV viral copies were higher (Fig 6F and 6G). This suggests that HSF2 modulates EBV gene expression in gastric adenocarcinoma cells, which is consistent with our findings in KSHV-infected cells.

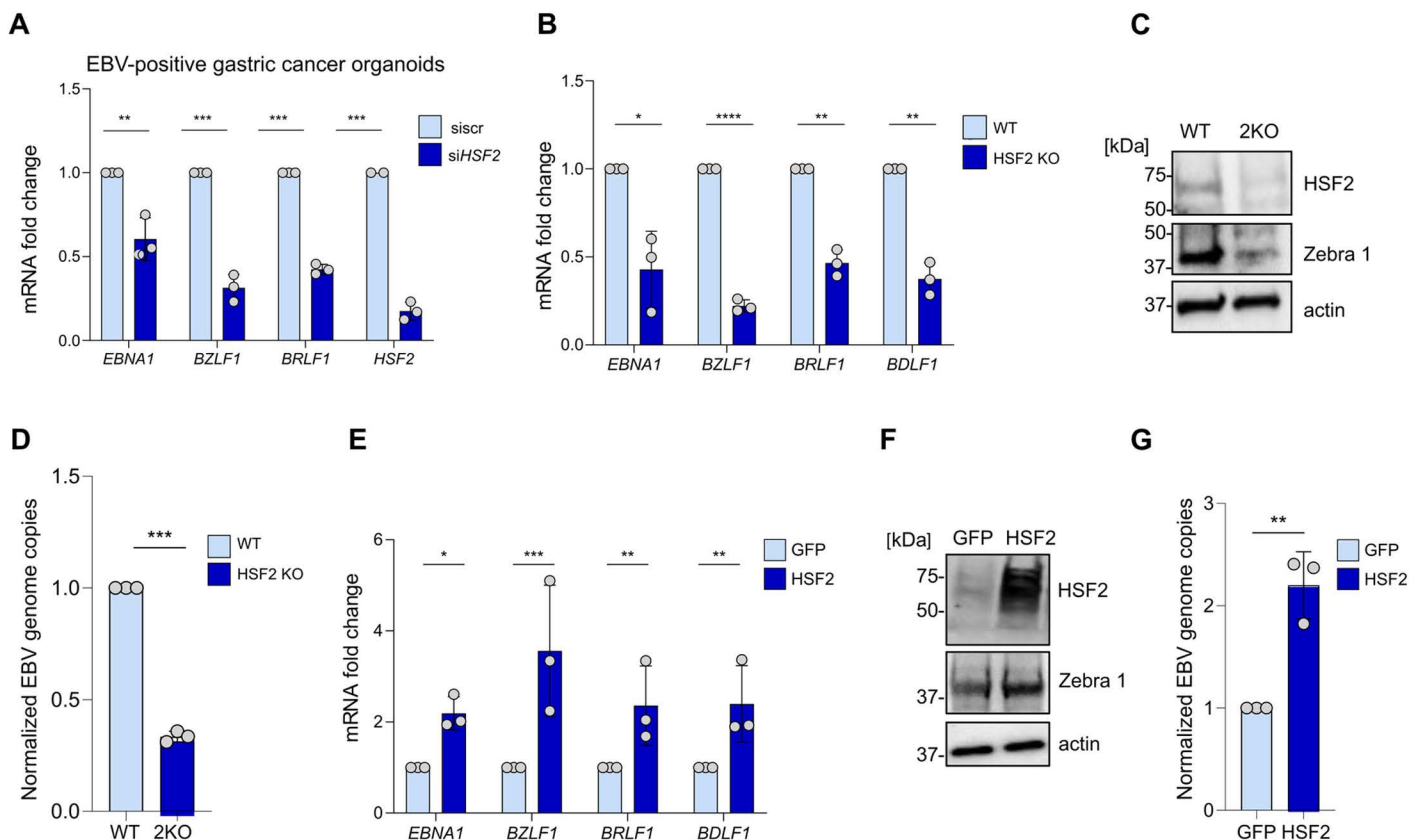


**Fig 6. HSF2 is a positive regulator of EBV spontaneous lytic cycle in gastric epithelial cells.** (A) patient-derived EBV-positive gastric adenocarcinoma cells were transfected with control, scramble (sisr) siRNA or siRNA targeting HSF2 and the levels of the indicated viral transcripts were measured by RT-qPCR. *Actin* was used as internal control. Bars represent the average and error bars the SD across three independent experiments, data points are indicated as grey circles. (B, C, D) Gastric adenocarcinoma AGS cell lines stably infected with EBV and with lentivirus expressing a CRISP/Cas9 and a sgRNA targeting HSF2 (indicated as 2KO). (B) Cells were analyzed for the indicated EBV viral transcripts by RTqPCR. Bars represent the average and error bars the SD across three independent experiments, data points are indicated as grey circles. (C) Cells were analyzed by immunoblot for HSF2 and the viral protein Zebra 1 (encoded by the BZLF1 gene) proteins, *actin* was used as a loading control. Representative images are shown, molecular weight in kDa is shown on the left. (D) DNA was extracted, and the intracellular viral genome copies were measured. Bars represent the average and error bars the SD across three independent experiments, data points are indicated as grey circles. (E, F, G) Gastric adenocarcinoma AGS cell lines stably infected with EBV and with lentiviruses expressing either HSF2 or GFP. (E) Cells were analyzed for the indicated EBV viral transcripts by RTqPCR with *Actin* as internal control. Bars represent the average and error bars the SD across three independent experiments, data points are indicated as grey circles. (F) Cells were analyzed by immunoblot for HSF2 and Zebra protein levels (encoded by the BZLF1 gene) proteins, *actin* served as a loading control. Representative images are shown, molecular weight in kDa is shown on the left. (G) DNA was extracted, and the intracellular viral genome copies were measured. Bars represent the average and error bars the SD across three independent experiments, data points are indicated as grey circles.

<https://doi.org/10.1371/journal.ppat.1013108.g006>

We next explored whether HSF2 might influence EBV lytic reactivation by modulating BRLF1 promoter, coding for the EBV RTA protein. We used the JASPAR database to screen the BRLF1 promoter upstream of the gene coding for EBV RTA gene and did not find any HSF2 binding element. Given the variations not only in viral gene expression but also the remarkable changes in the intracellular EBV genome copies upon HSF2 perturbations, we tested the hypothesis that HSF2 would regulate BZLF1 promoter, upstream of the gene coding for ZTA, responsible for early lytic genome replication. For this purpose, we utilized the JASPAR software to screen the BZLF1 promoter for HSF2-binding sites. Interestingly, we found an HSE motif consisting of two consecutive repeats of the pentameric nGAAn consensus sequence upstream of the BZLF1 TSS (Fig 7A, HSE location highlighted in yellow). Prompted by this finding, we examined whether endogenous HSF2 would bind to the BZLF1 promoter in AGS BX1 cells. We observed a significant increase in HSF2

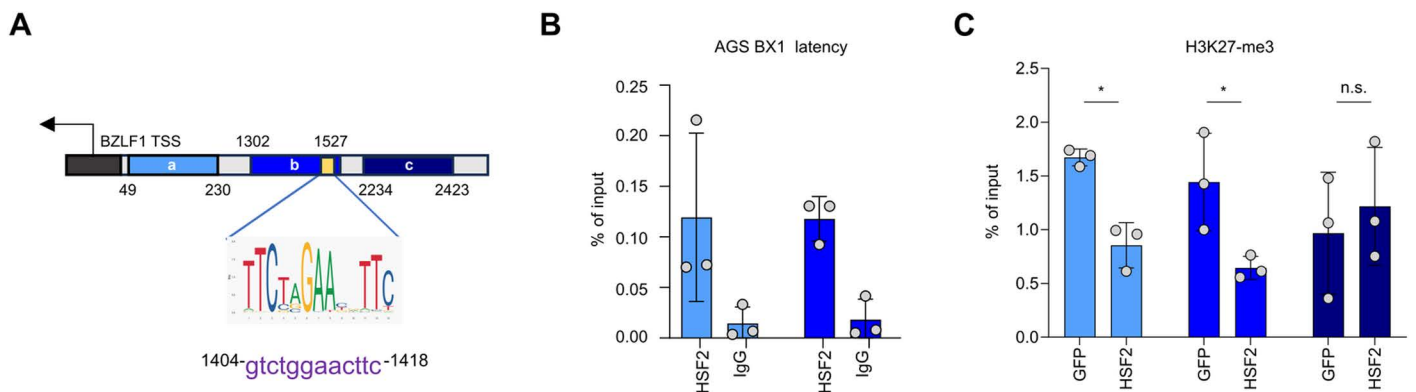


**Fig 7. HSF2 binds to the BZLF1 promoter and remodels the chromatin locally.** (A) Schematics of the EBV-BZLF1 promoter region, transcription start site (TSS and black arrow) and HSF2 binding site (yellow box) are shown. The regions amplified in CHIP-qPCR (blue segments) and their nucleotide positions are labeled. Below the HSE consensus logo and the corresponding nucleotide sequence within the BZLF1 promoter are shown. (B) CHIP-qPCR analysis of endogenous HSF2 binding to the BZLF1 promoter regions expressed as % of input in AGS BX1 cells. (C) HSF2 or GFP control overexpressing AGS BX1 cells were used to immunoprecipitated H3K27-me3 followed by RTqPCR for the indicated primers targeting different regions of the BZLF1 promoter. The bars are colored according to the schematic in (A). Bars represent the average and error bars the SD across three independent experiments, data points are indicated as grey circles.

<https://doi.org/10.1371/journal.ppat.1013108.g007>

binding in the most proximal promoter region and in the distal region where the HSE was present (Fig 7B). It has been previously reported that the EBV BZLF1 promoter, like the KSHV ORF50 promoter, displays bivalent chromatin marks that allows for efficient and quick lytic reactivation upon appropriate trigger [71]. These observations led us to ask whether the local epigenetic landscape at the BZLF1 promoter would be different in AGS BX1 cells overexpressing HSF2 than in parental cells harboring control GFP. We performed CHIP-PCR to assess H3K27-me3 distribution in one region proximal to the BZLF1 TSS and two more distal regions, with one of them harboring the putative HSF2-binding motif (Fig 7C). We observed significantly lower levels of the H3K27-me3 repressive chromatin mark in the proximal region and in the distal region harboring the HSE motif within the BZLF1 promoter (Fig 7C).

In conclusion, these results indicated that HSF2 regulates EBV gene expression and viral genome copies in gastric cancer cells. HSF2 binds to the BZLF1 promoter and remodels the local chromatin landscape towards a more transcriptionally permissive status at the BZLF1 promoter.

## Discussion

The heat shock factor family of transcription factors is composed of seven HSF members, of which only HSF1 and partially HSF2 are involved in maintaining protein homeostasis under external stress [72]. HSF1 is the master regulator of the heat shock response, and it interacts with HSF2 to drive expression of specific genes [25,26,72]. Beyond mitigating damage caused by proteotoxic stress, HSF family members are also required for cell differentiation and development of specific organs and their malfunction leads to diverse pathological conditions [21]. While the functions of HSF1 have been extensively studied, HSF2 has remained less explored. In this study, we interrogated the role of HSF2 in gamma-herpesvirus reactivation. We show that HSF2 maintains a permissive transcriptional environment in the chromatin of key viral promoters that facilitates downstream lytic gene expression in both oncogenic human gamma-herpesviruses, EBV and KSHV. HSF2 modulates viral gene expression in physiologically relevant models of viral-mediated oncogenesis, including primary KLEC and EBV-positive, patient-derived gastric cancer organoids.

The tight interconnection and cross-regulation between HSF1 and HSF2, has provoked us to ask whether HSF1 would contribute to the molecular processes regulated by HSF2. It is worth noting that the interdependence between HSF2 and HSF1 has been examined especially in HSF2-focused studies, while HSF1 research tends to ignore the potential impact

of HSF2. This implies that the functions and roles of HSF2 in several cellular and viral processes could be underestimated, warranting further investigations. In this study we found that HSF2 regulates the ORF50 expression independently of HSF1. This is consistent with the architecture of the HSE located at the ORF50 promoter. The variation in the affinity of HSF1 or HSF2 to the DNA depends on several factors including the HSE architecture, *i.e.*, length and orientation of the pentameric nGAAn sequence repeats. *In vitro* and *in vivo* studies have elegantly shown a predilection by HSF2 for shorter HSEs, with only two or three repeats of the pentameric motif, whereas HSF1 preferentially binds cooperatively to longer HSEs [31,46]. Accordingly, the ORF50 promoter, harboring a triad of the nucleotide consensus sequence, represents a better target for HSF2 rather than for HSF1 binding. Similarly, we detected a shorter HSE motif on the BZLF1 promoter and observed endogenous HSF2 binding. Our data indicate that HSF2 binding extends beyond the canonical HSEs, spanning a broader region on both the KSHV ORF50 and EBV BZLF1 promoters. This suggests that HSF2 may be recruited to these viral loci in coordination with other binding partners, potentially forming a larger regulatory complex. Such cooperative interactions could contribute to the observed local chromatin remodelling and to the fine-tuning of the viral reactivation process. Further investigation is needed to identify potential co-factors facilitating HSF2 recruitment and to elucidate their roles in modulating herpesviral gene expression.

Cells ectopically expressing HSF2 displayed a change in the epigenetic landscape at the ORF50 and BZLF1 promoter regions, in which the levels of the repressive H3K27-me3 chromatin mark were significantly reduced. It has been previously demonstrated that the ORF50 and BZLF1 promoters bear epigenetic features of bivalent chromatin, exhibiting both activating and repressive marks [11,48,71]. This poised chromatin state, first identified in lineage-specific promoters of embryonic stem cells (ESCs), was subsequently found at promoters of genes important for somatic development (reviewed in [50,73]). Bivalent chromatin state is also retained in germ cells from fetal stages through meiosis and gametogenesis [74]. HSF2 expression is enriched in testis, where it displays a nuclear localization and its genomic depletion leads to defects in spermatogenesis in mice [75–79]. Although no direct evidence is available to date, it is possible that HSF2 would be a mediator of chromatin remodeling by regulating the levels of H3K27-me3 at target poised promoters, especially during differentiation processes.

It was previously shown that HSF2 binds to the HSP70 promoter [22,59], and this binding is thought to prevent chromatin condensation, keeping this genomic locus accessible for rapid activation in case of acute stress [80]. The HSF2-mediated priming of the HSP70 promoter is important during mitosis when the transcription is dramatically repressed and the chromatin tightly condensed [59]. Intriguingly, a few genes escape this silencing and one of them is the gene encoding HSP70. During mitosis, in case of acute stress, HSF2 is released from the HSP70 promoter, making it accessible to the more potent transactivator HSF1 [22,59]. The role of HSF2 at the ORF50 promoter in latent cells shows similarities to its function at the HSP70 promoter. In both cases, HSF2 binds to target promoter regions when the genomic chromatin is repressed. Furthermore, upon lytic reactivation HSF2 is degraded, making the ORF50 promoter accessible to RTA, its main activator. This similarity suggests that HSF2 may play a conserved role in facilitating promoter accessibility, preparing the ORF50 promoter for activation by RTA, analogously to how it primes the HSP70 promoter for HSF1.

Our results demonstrated that when the lytic cycle is triggered in KSHV-infected cells, HSF2 is released from the ORF50 promoter and undergoes proteasomal degradation. Similarly, following its dissociation from the HSP70 promoter, HSF2 is subjected to ubiquitin-mediated proteasomal degradation. In mitotic cells, this process is catalyzed by the anaphase promoting complex APC/C that was found to be the specific E3 ubiquitin ligase in this pathway [58]. Other herpesviruses, like HCMV, induce the disruption of the APC/C, a process required for efficient viral replication [81]. In contrast, KSHV lytic cycle does not interfere with the APC/C activity and hence, this E3 ligase may contribute to HSF2 degradation in this setting [82]. However, some KSHV lytic proteins, including RTA, feature E3 ubiquitin-ligase activity [60] and our results suggest that ectopic RTA expression in uninfected cells can reduce HSF2 protein levels. This suggests that, specifically during the lytic cycle, RTA could also be involved in HSF2 degradation. This advances our understanding of the complex interaction between herpesviruses and the host cellular machinery suggesting that subsets of host proteins implicated in lytic reactivation are targeted for degradation after completing their tasks.

Recent transcriptomic profiling experiments have reproducibly shown that in tumors of epithelial and endothelial origin, like EBVaGC, NPC and KS, the viral gene expression landscape includes both latent genes and a scattered repertoire of lytic genes [7,83–85]. This unusual expression pattern cannot be ascribed to any of the canonical viral expression programs, and it has been referred to as permissive latency, a “leakage” of lytic genes within the latent program, and recently it has been defined as a “mixed” expression program [8,9,84,85]. These observations are further reinforced by the independent detection of multiple viral lytic proteins in tumor biopsies of KS lesions. Lytic proteins like K8.1 and K15 have been detected together with a robust expression of the lytic viral tegument gene ORF75 [38,84,86,87]. Interestingly, the lytic expression pattern found in KS lesions did not correlate with the levels of plasma viremia, suggesting that even in the lesions with higher levels of lytic gene expression, KSHV infection was not productive [87]. This implies, at least in these tumors, the presence of complex patterns of viral gene expression different from the classically mutually exclusive latent vs. lytic programs. Hence, we propose that HSF2 by promoting ORF50 gene expression, would contribute to the “leakage” of downstream lytic transcripts in latently infected cells within these tumors. In this context, HSF2 could represent a pro-oncogenic host factor supporting the expression of viral lytic oncogenes outside of the traditional productive lytic cycle.

Stress is a well-established trigger of herpesviral reactivation, serving as a viral survival strategy to enhance transmission under conditions that threaten host viability. Proteotoxic stress induces molecular chaperones such as HSP90 and various HSP70 isoforms, which are essential for efficient lytic replication, virion assembly, and release. While stress-induced activation of heat shock factors (HSFs) can contribute to this process, HSF2 itself is not broadly upregulated during acute stress response and regulates only a small subset of stress-responsive genes independently of HSF1 under these conditions [27]. Bortezomib (BTZ), an FDA-approved anticancer drug that induces proteotoxic stress, is currently the best characterized HSF2 activator. It has been recently reported that during BTZ treatment, HSF1 is the key regulator of HSF2 expression [44]. Notably, BTZ has been shown to trigger lytic reactivation of KSHV and EBV [88,89], suggesting that HSF2 upregulation in this context may contribute to viral reactivation.

Collectively, our findings provide evidence of a novel role for HSF2 as a previously underestimated, common player in EBV and KSHV gene regulation. Specifically, we show that HSF2 induces a more permissive chromatin environment at the RTA and BZLF1 promoters and the downstream expression of lytic genes prior to the initiation of the lytic cycle. These results add HSF2 to the complex host molecular network which controls gamma herpesviral latent-to-lytic switch, a process strongly connected to oncogenesis. Furthermore, this study uncovers new clues on the function of HSF2 at poised gene promoters, which could advance our understanding of its role in cellular differentiation processes.

## Materials and methods

### Cell lines

HEK293FT (Thermo Fisher Scientific, R70007; RRID:CVCL\_6911) and U2OS cells WT and *Hsf2*<sup>-/-</sup> (2KO) [22,90] cells were maintained in Dulbecco’s modified Eagle media (DMEM) supplemented with 10% heat-inactivated FBS (GIBCO) 1% L-glutamate and 1% Penicillin/streptomycin.

iSLK.219 [39], were maintained in DMEM media supplemented with 10% heat-inactivated FBS (GIBCO) 1% L-glutamate and 1% penicillin/streptomycin in the presence of puromycin (0.01 mg/mL) (A11138-03, GIBCO), hygromycin B (1.2 mg/mL) (10687010, Invitrogen) and G418 (0.8 mg/mL) (G8168, Sigma Aldrich). When plated for experiments or virus production antibiotics were not supplied to the media.

Primary human dermal lymphatic cells (LEC) (C-12216, PromoCell) were grown in endothelial basal media (CC-3162, Lonza) supplemented with EGM-2 MV Microvascular Endothelial SingleQuots (CC-4176).

AGS BX1 were maintained in Roswell Park Memorial Institute (RPMI) 1640 (R5886-500, Sigma-Aldrich) media supplemented with 10% heat-inactivated FBS (GIBCO) 1% L-glutamate and 1% penicillin/streptomycin in the presence of puromycin (5 µg/mL) and G418 (0.3 mg/mL) for the antibiotic selection. AGS BX1 cell lines were a kind gift from Maria Masucci (Karolinska Institutet, Sweden).

Gastric cancer primary cells were obtained from Silvia Giordano (University of Turin) and characterized as reported in [69]. Cells were grown in ISCOVE media (GIBCO) supplemented with 10%FBS and 1% penicillin/streptomycin on collagen (rat collagen type 1 solution, Sigma Aldrich) coated plates [69].

All cells were maintained under standard conditions (37C, 5% CO<sub>2</sub> and in a humidified environment)

### **KSHV reactivation and virus production**

iSLK.219 cells were seeded to reach a 70–80% confluency and the next day the lytic cycle was induced with doxycycline (1 ug/mL). To demonstrate the efficiency of reactivation images were taken with ZOE Fluorescent Cell Imager. For virus production, media was harvested 96 hours post-reactivation and centrifuged at 1000 RCF at 4°C for 30 minutes. rKSHV.219 particles then were concentrated with PEG-it (LV825A-1, System Biosciences) according to the manufacturer's instructions.

### **Generation of stably KSHV infected cells**

Klec were generated as reported in [38]. Briefly, LEC cells were seeded in a 6-well plate until a confluence of 60–70% was reached. The cells were infected with rKSHV.219 using polybrene diluted in the EBM2 media followed by spinoculation at 450g for 30 minutes at RT.

U2OS rKSHV.219 and HEK.219 cells were generated by infecting U2OS and HEK.293FT cells with rKSHV.219 virus by spinoculation at 450g, for 30 min at RT. One day post-infection puromycin selection (5 µg/mL) was initiated for U2OS. For HEK.219 puromycin selection (1.25 µg/mL) was initiated 72h post-infection. Cells were maintained in selection antibiotics-containing media. Selection antibiotics were not added when cells were plated for experiments.

### **Lentiviral production and lentiviral transduction**

HEK293FT cells were plated on a T75 flask to reach 60–70% confluency the next day. One day after plating, cells were transfected with the pLP1, pLP2 and VSVg plasmids (Addgene) and with the lentiviral plasmid carrying the gene of interest using lipofectamine 3000 (L3000008, Invitrogen) according to the manufacturer's instructions. Media was changed the next day and lentivirus-containing media was harvested at 72h and 96h after transfection. Lentivirus particles were concentrated with PEG-it (LV825A-1, System Biosciences) according to the manufacturer's instructions. Lentiviral expression vectors were designed and purchased from VectorBuilder Inc. HSF2 knockout: hHSF2[gRNA#1151]; HSF2 overexpression and control: hHSF2[NM\_004506.3]; GFP: pLV[Exp-Puro-EF1A>EGFP [29].

Lentiviral transduction was performed on 60–70% cell layers by adding the lentivirus to fresh growth media in the presence of 8 ug/mL of polybrene followed by spinoculation at 450g for 30 minutes at RT.

### **Generation of stable cell lines**

1x10<sup>5</sup> AGS BX1 cells were plated in a 6-well plate and transduced with the indicated lentiviruses. Cells were maintained as a bulk culture and puromycin selection (5 µg/mL) was initiated 48h after transduction. Cells were maintained in selection antibiotics-containing media. Selection antibiotics were not added when cells were plated for experiments.

### **siRNA transfection**

U2OS rKSHV.219, iSLK.219, KLEC cells were transfected with either 10 pmol/mL siRNA ON-target plus smart pool targeting HSF2 (Dharmacon, L-011874-00-0020), HSF1 (Dharmacon, I-012109-02-0005) or control, scrambled siRNA (Dharmacon, D-001810-10) in presence of the lipofectamine RNAiMAX transfection reagent (13778-075, Invitrogen) according to the instructions provided by the manufacturer. The siRNA used is a mixture of 4 different siRNA provided as a single reagent, thus ensuring both higher potency and specificity than an individual siRNA. The efficacy of HSF2 and HSF1 silencing was confirmed by immunoblotting.

### Transfection and luciferase reporter assay

$3 \times 10^4$  HEK-293FT cells/well were seeded in a 96-well white plate. The next day cells were co-transfected in triplicate with 50 ng of the reporter plasmids, or the corresponding control vector and either 100 ng of HSF2 or control GFP expressing plasmids and where indicated, pFuW-Myc-ORF50 plasmid [91] in the presence of Fugene HD (E2311, Promega) according to the manufacturer's instructions. 48 hours after transfection cells were lysed in 50  $\mu$ l/well of ONE-GloLuciferase Assay Reagent (E6110, Promega). The luciferase activity was measured by total counts acquired using the HIDEX sense 425-301i plate reader and software (Hidex).

The following reporter plasmids were used in this study: pGL2-basic (Promega); pGL2-ORF50 pGL3-basic (Promega); pGL3-7XTR; pGL3-Orilyt; pGL3-ORF45 and pGL3-K8.1 (provided by T.F. Schulz, Hannover Medical School, Germany).

For each experimental setting, three independent experiments were performed in triplicates. The transfection efficiency, for each condition, was assessed with immunoblotting.

### Quantification of intracellular viral genome copies

DNA was isolated using QIAamp DNA Micro Kit (56304, Qiagen) and analyzed by qPCR using primers for genomic actin (5'-AGAAAATCTGGCACCCACACC-3'; 5'-AACGGCAGAAGAGAGAACCA-3') and genomic EBV copies were detected by amplification of a portion of the gp85 region (5'-TGTGGATGGGTTTCTTGGGC-3'; 5'-TGGTCAGCAGCAATAGTGAAGC-3').

### Inhibitor treatment

$0.5 \times 10^5$  iSLK.219 cells/well were seeded in a 24-well plate. On the next day, cells were reactivated with Doxycycline. 22 hours post reactivation cells were either treated with the protease inhibitor MG-132 (2194S, Cell Signaling Technology) used with a concentration of 20  $\mu$ M or an equal volume of DMSO used as negative control. 24 hours post reactivation cells were harvested and stored at  $-80^\circ\text{C}$  for further analysis.

### qRT-PCR

RNA was isolated with RNeasy Mini Kit (74136, QIAGEN) according to the manufacturer's instructions. The amount of RNA was quantified using a NanoDrop 2000 spectrophotometer (ThermoFisher Scientific), and for each sample, 900 ng of RNA were reverse transcribed using the iScript cDNA Synthesis Kit (#1708891, Bio-Rad). SensiFAST SYBR Hi-ROX kit (BIO-92020, Meridian Bioline) was used in the qPCR reactions, which were performed using a QuantStudio 3 Real-Time PCR system (Applied Biosystems, Thermo Fisher Scientific). Actin or 18S were used as housekeeping genes for the normalization of all other gene expression. Samples were run in triplicates and each experiment was done at three independent times. The primer sequences are listed in [Table 1](#).

### ChIP-PCR

SimpleChip Enzymatic Chromatin IP Kit (Magnetic Beads) (#91820:9003, Cell Signaling Technology) was used according to the manufacturer's instructions. For each immunoprecipitation (IP), the chromatin from  $6 \times 10^5$  iSLK.219 or AGS BX.1 cells was crosslinked with 1% formaldehyde.

For the identification of HSF2 association on specific regions of the KSHV ORF50 promoter 2  $\mu$ L of antibodies against HSF2 (SFI58) [22] and as control normal Rabbit IgG (#2729, Cell Signaling Technology) were used. For the quantification of histone markers tri-methyl-histone H3(K4) (#9751, Cell Signaling technology), tri-methyl-histone H3(K27) (#9733T, Cell Signaling technology) and normal Rabbit IgG (#2729, Cell Signaling Technology) were used at the concentration of 1:150 as per manufacturer's recommendation.

**Table 1. Primers used in RTqPCR.**

Primers	Forward	Reverse
BDLF1	5'-GCACCTCCTCTGCTATGGGC-3'	5'-TGATACTACCAAGATTGTTCCAGG-3'
BRLF1	5'-CCT GTC TTG GAC GAG ACC AT-3'	5'-AAGGCCTCCTAAGCTCCAAG-3'
BZLF1	5'-ACGACGCACACGGAAACC-3'	5'-CTTGGCCCGGCATTTTCT-3'
EBNA1	5'-GGTGGAGACCCGGATGAT G-3'	5'-GGTCGTGGACGTGGAGAA AA-3'
hHSF1	5'-TCGAACACGTGGAAGCTGT-3'	5'-3'CAAGCTGTGGACCCTCGT
hHSF2	5'-GGAGGAAACCCACACTAAG-3'	5'-ATCGTTGCTCATCCAAGACC-3'
Actin	5'-TCACCCACACTGTGCCATCTACGA-3'	5'-CAGCGGAACCGCTCATTGCCAATGG-3'
K8.1	5'-AAAGCGTCCAGGCCACCACAG-3'	5'-GGCAGAAAATGGCACACGGTTAC-3'
ORF45	5'-CCTCGTCGTCGTAAGGTG-3'	5'-GGGATGGGGTTAGTCAGGATG-3'
ORF50	5'-CACAAAATGGCGCAAAGATGA-3'	5'-TGGTAGAGTTGGGCCTTCAGTT-3'
ORF57	5'-TGGACATTTATGAAGGGCATCCTA-3'	5'-CGGGTTCGGACAATTGCT-3'
ORF73	5'-ACTGAACACACGGACAACGC-3'	5'-CAGGTTCTCCCATCGACG-3'
18S	5'-GCAATTATCCCCATGAACG-3'	5'-GGGACTTAATCAACGCAAGC-3'

<https://doi.org/10.1371/journal.ppat.1013108.t001>

**Table 2. Primers used in CHIP-PCR.**

Primers	Forward	Reverse
ORF50 promoter pair a	5'-TTTACTGCTCCAACAGGCCC-3'	5'-AGGCCATTGACAGAACTCCG-3'
ORF50 promoter pair b	5'-TGTGCGTTTATGAGCGGAGT-3'	5'-GCCAGGGTGTGTTGCTACTA-3'
ORF50 promoter pair c	5'-ATTGGGGACGGAAGCCTCTA-3'	5'-CCCACAGGACAAGCTGATGT-3'
ORF50 promoter pair d	5'-TACGGGTCCTGGCCTAAGAT-3'	5'-GGACGACCGGGATCTGTTAC-3'
ORF50 promoter pair e	5'-CCACCACATCAGCTTGTCT-3'	5'-CAGACGGTCTTTAGGGGCAC-3'
ORF50 promoter pair f	5'-AACCAATCCCAGCCAAGTCC-3'	5'-AGTGTGGATCCGCAATGTCA-3'
BZLF1 promoter pair a	5'-GCTCACGTAGCTCCTCTGTC-3'	5'-GTGGGTGTTACCTATCCCG-3'
BZLF1 promoter pair b	5'-GTGGCTCAGGTCCATCTGTC-3'	5'-ATGAACCGGTCCGATCCCTA-3'
BZLF1 promoter pair c	5'-TGCTGGAAGACACCATCGTC-3'	5'-GTCTGTCTTGGCGCAGTTTC-3'
hHFSF70	5'-GACTCTGGAGATTCTGA-3'	5'-TCCCTTCTGAGGCAATC-3'

<https://doi.org/10.1371/journal.ppat.1013108.t002>

The experiments were performed at least three independent times. Isolated and purified DNA was amplified by quantitative real-time PCR using the indicated primer pairs listed in [Table 2](#).

### Immunoblotting

Cells were lysed in 3x Laemmli lysis buffer (30% glycerol, 187.5mM SDS, 3% Tris-HCl, 0.015% bromophenol blue, 3% β-mercaptoethanol), and boiled for 5 minutes at 95 °C and then resolved on 7.5% or 4–20% Mini-PROTEAN TGX Stain-Free Precast Gels (Bio-Rad) and transferred onto an Amersham Protran 0.45 nitrocellulose membrane (Cytiva). The membranes were blocked with 5% milk-PBS-Tween20 to detect the proteins of interest. The following primary antibodies were diluted in 5% milk-PBST and used for immunoblotting with a 1:1000 dilution for the anti-HSF2 (HPA031455, Sigma-Aldrich) and anti-HSF1 (SMC-118C, StressMarq Biosciences), 1:500 dilution for anti-K8.1 (sc-65446, SantaCruz); anti-K-bZIP (sc-69797, SantaCruz); 1:250 anti-LANA (AB4103, abcam); anti-actin (A4700, Sigma-Aldrich); anti-alpha-tubulin (12G10, DSHB) and incubated overnight at 4°C. After three rounds of washing in PBST the following Horseradish peroxidase-conjugated secondary antibodies were diluted in 5% milk-PBST and used with at a 1:10000 dilution anti-rabbit (W4018, Promega), 1:5000 anti-mouse (W402B, Promega), 1:3000 anti-Rat (ab97057, abcam) and incubated at room

temperature for 1 hour. After 3 rounds of washing in PBST luminescent signal was revealed with Super Signal West Pico PLUS Chemiluminescent Substrate (34580, Thermo Scientific) using the chemiluminescent program of detection on the iBrightCL1000. Experiments were done at least two independent times; representative experiments are shown. Equal loading of the independently generated blots was ensured by Ponceau-S staining.

### Immunofluorescence

iSLK.219 cells plated on coverslips were either treated with Doxycycline or left untreated. 24-hour post reactivation cells were fixed with 4% paraformaldehyde for 10 min at RT and washed three times with PBS. Cells were then permeabilized and stained with DAPI (1  $\mu\text{g}/\text{mL}$ ) dissolved in 0.5% Triton X-100 and 3 mM EDTA in PBS in the dark, at room temperature, for 10 min. The cells were then washed three times with PBS and blocked with 1% BSA in TBST for 1 h at RT and incubated with primary antibodies overnight at 4°C. The primary antibodies were diluted in 1% BSA in TBST: 1:100 anti-HSF2 (HPA031455, Sigma-Aldrich) and 1:200 anti-tri-methyl-histone H3(K4) (9751T, Cell Signaling). After primary antibody incubation, cells were washed with PBS incubated with secondary antibodies for 1 hour at RT. The following secondary antibodies were diluted in 1% BSA-TBST; 1:500 anti-rabbit Alexa Fluor 547(A-21244, Invitrogen). Next, the cells were washed with PBS and with MQ-water and then mounted with VECTASHIELD mounting medium (H-100, Vector Laboratories). Coverslips were imaged with Zeiss LSM 880 microscope using a 40X objective. Acquired images are shown as maximum intensity projections. The integrated nuclear intensity was used to compare the HSF2 levels between the latent and lytic-infected cells.

For viral titre quantification, U2OS cells were plated on a 96 clear bottom black well-plate (655090, Greiner) infected with serial dilution of supernatant from KLEC treated as indicated for 24h. Cell were then fixed and stained with DAPI. The primary antibodies were diluted in 1% BSA in TBST: 1:200 anti-LANA (AB4103, abcam) and the secondary antibody used was anti-rat Alexa Fluor 647 (A-21247, Invitrogen) diluted 1:500. Stained cells were imaged with an HT microscope using a 10X objective. Cells positive for LANA were identified by subtracting the background intensity from uninfected cells (stained with LANA antibody) and expressed as percentage of LANA positive cells. The number of LANA-positive cells were quantified over the total amount of nuclei (number of nuclei) using Cell Profiler (<http://cellprofiler.org>)

### Statistical analysis

Data were analyzed with Prism GraphPad 8. Unless differently stated in the legend, the graphs show the single values of each biological replicate, the mean and the error bars indicate the SD across the biological replicates. Ordinary one-way ANOVA followed by Dunnett correction for multiple comparisons or two-tailed paired *t* test were performed to assess the statistical significance of the differences between samples. \*:  $p < 0.05$ ; \*\*:  $p < 0.01$ ; \*\*\*:  $p < 0.001$ ; n.s.: non-significant.

### Supporting information

**S1 Fig. HEK.219 cells were treated with the indicated siRNAs for 24h.** (A) Cells were harvested, and protein levels were analyzed by immunoblot, actin was used as a loading control, molecular weight in kDa is shown on the left side of each blot. (B) RNA was extracted and analyzed for the expression of the indicated viral targets. (TIF)

**S2 Fig. (A–D) Representative immunoblots for the reporter assays shown in Fig 4A–D.** HEK293FT cells were transfected with the indicated plasmids for 24h and after luciferase reporter activity measurement, the protein lysate was analyzed by immunoblot for HSF2 expression, longer membrane exposures are shown to demonstrate endogenous HSF2 expression in GFP transfected cells. Actin was used as loading control. (E) Immunoblot analysis for HSF1 and HSF2 in U2OS rKSHV.219 cells overexpressing GFP or HSF2 and transfected with either control (scr) siRNA or an siRNA targeting HSF1 for 48 hours. Actin was used as a loading control. (F) RTqPCR analysis of cells treated as in (E) for *ORF50* gene, *actin* was used as internal control. (TIF)

**S3 Fig. (A and B) ChIP-qPCR analysis of HSF2 binding to the indicated KSHV genomic regions expressed as % of input in KSHV infected latent (A) and lytic (B) cells.** (C and D) ChIP PCR analysis of the indicated histone H3 modification in latent iSLK.219 cells overexpressing HSF2 or GFP. Bars represent the average, and the error bars the SD across three independent experiments, data points are indicated as circles. (E) Immunoblot analysis of iSLK.219 cells overexpressing either HSF2 or GFP control. Actin was used as a loading control.

(TIF)

**S4 Fig. (A) Confocal representative images and (B) quantification of the H3me3K4 integrated intensity in n > 100 cells in iSLK.219 either latent or induced to the lytic cycle with doxycycline for 24h (indicated as lytic).** (C) Transcript analysis of *ORF57* gene in iSLK.219 cells reactivated with doxycycline (Dox) for the indicated hours. *Actin* was used as internal control. Bars represent the average and error bars of the SD across three independent experiments, data points are indicated as grey circles.

(TIF)

## Acknowledgment

We thank the members of the Sistonen research group for critical discussions. Prof. Maria Masucci, Prof. T.F. Schulz and Prof. Päivi M. Ojala are acknowledged for providing plasmids and cell lines. The staff of the facilities of the Turku Screening Unit, a member of the Biocentre Finland Drug Discovery and Chemical Biology Network and EU-Openscreen ERIC and Turku Bioscience Center are acknowledged for technical support.

## Author contributions

**Conceptualization:** Lea Sistonen, Silvia Gramolelli.

**Data curation:** Lorenza Cutrone, Silvia Gramolelli.

**Formal analysis:** Lorenza Cutrone, Silvia Gramolelli.

**Funding acquisition:** Lorenza Cutrone, Lea Sistonen, Silvia Gramolelli.

**Investigation:** Lorenza Cutrone, Hedvig Djupenström, Jasmin Peltonen, Simona Corso, Silvia Giordano, Silvia Gramolelli.

**Methodology:** Lorenza Cutrone, Jasmin Peltonen, Elena Martinez Klimova, Silvia Gramolelli.

**Project administration:** Lea Sistonen, Silvia Gramolelli.

**Resources:** Simona Corso, Silvia Giordano.

**Supervision:** Silvia Gramolelli.

**Visualization:** Silvia Gramolelli.

**Writing – original draft:** Lorenza Cutrone, Silvia Gramolelli.

**Writing – review & editing:** Lorenza Cutrone, Hedvig Djupenström, Elena Martinez Klimova, Lea Sistonen, Silvia Gramolelli.

## References

- Goncalves PH, Ziegelbauer J, Uldrick TS, Yarchoan R. Kaposi sarcoma herpesvirus-associated cancers and related diseases. *Curr Opin HIV AIDS*. 2017;12(1):47–56. <https://doi.org/10.1097/COH.0000000000000330> PMID: 27662501
- Gaglia MM. Kaposi's sarcoma-associated herpesvirus at 27. *Tumour Virus Res*. 2021;12:200223. <https://doi.org/10.1016/j.tvr.2021.200223> PMID: 34153523
- Young LS, Rickinson AB. Epstein-Barr virus: 40 years on. *Nat Rev Cancer*. 2004;4(10):757–68. <https://doi.org/10.1038/nrc1452> PMID: 15510157
- Wong Y, Meehan MT, Burrows SR, Doolan DL, Miles JJ. Estimating the global burden of Epstein-Barr virus-related cancers. *J Cancer Res Clin Oncol*. 2022;148(1):31–46. <https://doi.org/10.1007/s00432-021-03824-y> PMID: 34705104
- Hutt-Fletcher LM. The long and complicated relationship between Epstein-Barr virus and epithelial cells. *J Virol*. 2017;91(1):e01677-16. <https://doi.org/10.1128/JVI.01677-16> PMID: 27795426

6. Huang W, Bai L, Tang H. Epstein-Barr virus infection: the micro and macro worlds. *Virology*. 2023;20(1):220. <https://doi.org/10.1186/s12985-023-02187-9> PMID: [37784180](https://pubmed.ncbi.nlm.nih.gov/37784180/)
7. Cancer Genome Atlas Research Network. Comprehensive molecular characterization of gastric adenocarcinoma. *Nature*. 2014;513(7517):202–9. <https://doi.org/10.1038/nature13480> PMID: [25079317](https://pubmed.ncbi.nlm.nih.gov/25079317/)
8. Gramolelli S, Ojala PM. Kaposi's sarcoma herpesvirus-induced endothelial cell reprogramming supports viral persistence and contributes to Kaposi's sarcoma tumorigenesis. *Curr Opin Virol*. 2017;26:156–62. <https://doi.org/10.1016/j.coviro.2017.09.002> PMID: [29031103](https://pubmed.ncbi.nlm.nih.gov/29031103/)
9. Gramolelli S, Schulz TF. The role of Kaposi sarcoma-associated herpesvirus in the pathogenesis of Kaposi sarcoma. *J Pathol*. 2015;235(2):368–80. <https://doi.org/10.1002/path.4441> PMID: [25212381](https://pubmed.ncbi.nlm.nih.gov/25212381/)
10. Lieberman PM. Epigenetics and Genetics of Viral Latency. *Cell Host Microbe*. 2016;19(5):619–28. <https://doi.org/10.1016/j.chom.2016.04.008> PMID: [27173930](https://pubmed.ncbi.nlm.nih.gov/27173930/)
11. Günther T, Grundhoff A. Epigenetic manipulation of host chromatin by Kaposi sarcoma-associated herpesvirus: a tumor-promoting factor? *Curr Opin Virol*. 2017;26:104–11. <https://doi.org/10.1016/j.coviro.2017.07.018> PMID: [28802146](https://pubmed.ncbi.nlm.nih.gov/28802146/)
12. Manners O, Murphy JC, Coleman A, Hughes DJ, Whitehouse A. Contribution of the KSHV and EBV lytic cycles to tumorigenesis. *Curr Opin Virol*. 2018;32:60–70. <https://doi.org/10.1016/j.coviro.2018.08.014> PMID: [30268927](https://pubmed.ncbi.nlm.nih.gov/30268927/)
13. Grundhoff A, Ganem D. Inefficient establishment of KSHV latency suggests an additional role for continued lytic replication in Kaposi sarcoma pathogenesis. *J Clin Invest*. 2004;113(1):124–36. <https://doi.org/10.1172/JCI17803> PMID: [14702116](https://pubmed.ncbi.nlm.nih.gov/14702116/)
14. Martin JN, Osmond DH. Kaposi's sarcoma-associated herpesvirus and sexual transmission of cancer risk. *Curr Opin Oncol*. 1999;11(6):508. <https://doi.org/10.1097/00001622-199911000-00013> PMID: [10550016](https://pubmed.ncbi.nlm.nih.gov/10550016/)
15. Sandhu PK, Damania B. The regulation of KSHV lytic reactivation by viral and cellular factors. *Curr Opin Virol*. 2022;52:39–47. <https://doi.org/10.1016/j.coviro.2021.11.004> PMID: [34872030](https://pubmed.ncbi.nlm.nih.gov/34872030/)
16. Davis DA, Shrestha P, Yarchoan R. Hypoxia and hypoxia-inducible factors in Kaposi sarcoma-associated herpesvirus infection and disease pathogenesis. *J Med Virol*. 2023 Sep;95(9):e29071.
17. Kalmar B, Greensmith L. Induction of heat shock proteins for protection against oxidative stress. *Adv Drug Deliv Rev*. 2009;61(4):310–8. <https://doi.org/10.1016/j.addr.2009.02.003> PMID: [19248813](https://pubmed.ncbi.nlm.nih.gov/19248813/)
18. Wan Q, Song D, Li H, Liang HM. Stress proteins: the biological functions in virus infection, present and challenges for target-based antiviral drug development. *Signal Transduct Target Ther*. 2020 Jul 13;5(1):125.
19. Lippé R Deciphering novel host–herpesvirus interactions by virion proteomics. *Front Microbiol*. 2012 [cited 2024 Oct 30] 3. <https://doi.org/10.3389/fmicb.2012.00181>
20. Baquero B, Whitehouse A. Hsp70 isoforms are essential for the formation of Kaposi's sarcoma-associated herpesvirus replication and transcription compartments. *PLOS Pathog*. 2015;11(11):e1005274.
21. Roos-Mattjus P, Sistonen L. Interplay between mammalian heat shock factors 1 and 2 in physiology and pathology. *FEBS J*. 2022;289(24):7710–25. <https://doi.org/10.1111/febs.16178> PMID: [34478606](https://pubmed.ncbi.nlm.nih.gov/34478606/)
22. Östling P, Björk JK, Roos-Mattjus P, Mezger V, Sistonen L. Heat shock factor 2 (HSF2) contributes to inducible expression of hsp genes through interplay with HSF1. *J Biol Chem*. 2007;282(10):7077–86. <https://doi.org/10.1074/jbc.M607556200> PMID: [17213196](https://pubmed.ncbi.nlm.nih.gov/17213196/)
23. Pessa JC, Joutsen J, Sistonen L. Transcriptional reprogramming at the intersection of the heat shock response and proteostasis. *Mol Cell*. 2024;84(1):80–93. <https://doi.org/10.1016/j.molcel.2023.11.024> PMID: [38103561](https://pubmed.ncbi.nlm.nih.gov/38103561/)
24. Sandqvist A, Björk JK, Akerfelt M, Chitikova Z, Grichine A, Vourc'h C, et al. Heterotrimerization of heat-shock factors 1 and 2 provides a transcriptional switch in response to distinct stimuli. *Mol Biol Cell*. 2009;20(5):1340–7. <https://doi.org/10.1091/mbc.e08-08-0864> PMID: [19129477](https://pubmed.ncbi.nlm.nih.gov/19129477/)
25. Joutsen J, Sistonen L. Tailoring of proteostasis networks with Heat Shock Factors. *Cold Spring Harb Perspect Biol*. 2019 Apr 1;11(4). <https://doi.org/10.1101/cshperspect.a034066>
26. Himanen SV, Sistonen L. New insights into transcriptional reprogramming during cellular stress. *J Cell Sci*. 2019;132(21):jcs238402. <https://doi.org/10.1242/jcs.238402> PMID: [31676663](https://pubmed.ncbi.nlm.nih.gov/31676663/)
27. Himanen SV, Puustinen MC, Da Silva AJ, Vihervaara A, Sistonen L. HSFs drive transcription of distinct genes and enhancers during oxidative stress and heat shock. *Nucleic Acids Res*. 2022;50(11):6102–15.
28. Smith RS, Takagishi SR, Amici DR, Metz K, Gayatri S, Alasady MJ, et al. HSF2 cooperates with HSF1 to drive a transcriptional program critical for the malignant state. *Sci Adv*. 2022;8(11):eabj6526.
29. Pessa JC, Paavolainen O, Puustinen MC, Hästbacka HSE, Da Silva AJ, Pihlström S, et al. Dynamic HSF2 regulation drives breast cancer progression by steering the balance between proliferation and invasion [Internet]. 2024 [cited 2024 Oct 30]. Available from: <https://doi.org/10.1101/2024.06.24.600354>
30. Duchateau A, de Thonel A, El Fatimy R, Dubreuil V, Mezger V. The “HSF connection”: Pleiotropic regulation and activities of Heat Shock Factors shape pathophysiological brain development. *Neurosci Lett*. 2020;725:134895. <https://doi.org/10.1016/j.neulet.2020.134895> PMID: [32147500](https://pubmed.ncbi.nlm.nih.gov/32147500/)
31. Sistonen L, Sarge KD, Phillips B, Abravaya K, Morimoto RI. Activation of heat shock factor 2 during hemin-induced differentiation of human erythro-leukemia cells. *Mol Cell Biol*. 1992 Sep;12(9):4104–11.

32. De Thonel A, Ahlskog JK, Daupin K, Dubreuil V, Berthelet J, Chaput C, et al. CBP-HSF2 structural and functional interplay in Rubinstein-Taybi neurodevelopmental disorder. *Nat Commun.* 2022;13(1):7002. <https://doi.org/10.1038/s41467-022-34476-2> PMID: [36385105](https://pubmed.ncbi.nlm.nih.gov/36385105/)
33. Huang JR, Arii J, Hirai M, Nishimura M, Mori Y. Human herpesvirus 6A nuclear matrix protein U37 interacts with heat shock transcription factor 1 and activates the heat shock response. *J Virol.* 2023;97(9):e00718-23.
34. Akter D, Biswas J, Miller MJ, Thiele DJ, Murphy EA, O'Connor CM, et al. Targeting the host transcription factor HSF1 prevents human cytomegalovirus replication in vitro and in vivo. *bioRxiv.* 2024. <http://biorxiv.org/lookup/doi/10.1101/2024.09.23.614483> [cited 2024 Nov 3]. PMID: [39386472](https://pubmed.ncbi.nlm.nih.gov/39386472/)
35. Wang F-W, Wu X-R, Liu W-J, Liao Y-J, Lin S, Zong Y-S, et al. Heat shock factor 1 upregulates transcription of Epstein-Barr Virus nuclear antigen 1 by binding to a heat shock element within the BamHI-Q promoter. *Virology.* 2011;421(2):184–91. <https://doi.org/10.1016/j.virol.2011.10.001> PMID: [22018489](https://pubmed.ncbi.nlm.nih.gov/22018489/)
36. Choi D, Park E, Kim KE, Jung E, Seong YJ, Zhao L, et al. The lymphatic cell environment promotes kaposi sarcoma development by prox1-enhanced productive lytic replication of kaposi sarcoma herpes virus. *Cancer Res.* 2020;80(15):3130–44.
37. Tuohinto K, DiMaio TA, Kiss EA, Laakkonen P, Saharinen P, Karnezis T, et al. KSHV infection of endothelial precursor cells with lymphatic characteristics as a novel model for translational Kaposi's sarcoma studies. *PLOS Pathog.* 2023 Jan 23; 19(1):e1010753. <https://doi.org/10.1371/journal.ppat.1010753> PMID: [36689549](https://pubmed.ncbi.nlm.nih.gov/36689549/)
38. Gramolelli S, Elbasani E, Tuohinto K, Nurminen V, Günther T, Kallinen RE, et al. Oncogenic herpesvirus engages endothelial transcription factors SOX18 and PROX1 to increase viral genome copies and virus production. *Cancer Res.* 2020;80(15):3116–29.
39. Myoung J, Ganem D. Generation of a doxycycline-inducible KSHV producer cell line of endothelial origin: maintenance of tight latency with efficient reactivation upon induction. *J Virol Methods.* 2011;174(1–2):12–21. <https://doi.org/10.1016/j.jviromet.2011.03.012> PMID: [21419799](https://pubmed.ncbi.nlm.nih.gov/21419799/)
40. Vieira J, O'Hearn PM. Use of the red fluorescent protein as a marker of Kaposi's sarcoma-associated herpesvirus lytic gene expression. *Virology.* 2004;325(2):225–40. <https://doi.org/10.1016/j.virol.2004.03.049> PMID: [15246263](https://pubmed.ncbi.nlm.nih.gov/15246263/)
41. Sun R, Lin SF, Gradoville L, Yuan Y, Zhu F, Miller G. A viral gene that activates lytic cycle expression of Kaposi's sarcoma-associated herpesvirus. *Proc Natl Acad Sci.* 1998;95(18):10866–71.
42. Kaul R, Purushothaman P, Uppal T, Verma SC. KSHV lytic proteins K-RTA and K8 bind to cellular and viral chromatin to modulate gene expression. *PLOS ONE.* 2019;14(4):e0215394. <https://doi.org/10.1371/journal.pone.0215394> PMID: [30998737](https://pubmed.ncbi.nlm.nih.gov/30998737/)
43. Liang Y, Ganem D. Lytic but not latent infection by Kaposi's sarcoma-associated herpesvirus requires host CSL protein, the mediator of Notch signaling. *Proc Natl Acad Sci.* 2003;100(14):8490–5.
44. Santopolo S, Riccio A, Rossi A, Santoro MG. The proteostasis guardian HSF1 directs the transcription of its paralog and interactor HSF2 during proteasome dysfunction. *Cell Mol Life Sci.* 2021;78(3):1113–29. <https://doi.org/10.1007/s00018-020-03568-x> PMID: [32607595](https://pubmed.ncbi.nlm.nih.gov/32607595/)
45. Manuel M, Rallu M, Loones M, Zimarino V, Mezger V, Morange M. Determination of the consensus binding sequence for the purified embryonic heat shock factor 2. *Eur J Biochem.* 2002;269(10):2527–37.
46. Kroeger PE, Morimoto RI. Selection of new HSF1 and HSF2 DNA-binding sites reveals differences in trimer cooperativity. *Mol Cell Biol.* 1994;14(11):7592–603. <https://doi.org/10.1128/mcb.14.11.7592-603.1994> PMID: [7935474](https://pubmed.ncbi.nlm.nih.gov/7935474/)
47. Amin J, Ananthan J, Voellmy R. Key features of heat shock regulatory elements. *Mol Cell Biol.* 1988;8(9):3761–9.
48. Günther T, Grundhoff A. The epigenetic landscape of latent Kaposi sarcoma-associated herpesvirus genomes. *PLoS Pathog.* 2010;6(6):e1000935. <https://doi.org/10.1371/journal.ppat.1000935> PMID: [20532208](https://pubmed.ncbi.nlm.nih.gov/20532208/)
49. Puri D, Gala H, Mishra R, Dhawan J. High-wire act: the poised genome and cellular memory. *FEBS J.* 2015 May;282(9):1675–91. <https://doi.org/10.1111/febs.13165> PMID: [25440020](https://pubmed.ncbi.nlm.nih.gov/25440020/)
50. Mas G, Blanco E, Ballaré C, Sansó M, Spill YG, Hu D, et al. Promoter bivalency favors an open chromatin architecture in embryonic stem cells. *Nat Genet.* 2018;50(10):1452–62. <https://doi.org/10.1038/s41588-018-0218-5> PMID: [30224650](https://pubmed.ncbi.nlm.nih.gov/30224650/)
51. Bergwell M, Park J, Kirkland JG. Differential modulation of polycomb-associated histone marks by cBAF, pBAF, and gBAF complexes. *Life Sci Alliance.* 2024;7(11):e202402715. <https://doi.org/10.26508/lsa.202402715> PMID: [39209535](https://pubmed.ncbi.nlm.nih.gov/39209535/)
52. Naro C, Antonioni A, Medici V, Caggiano C, Jolly A, De La Grange P, et al. Splicing targeting drugs highlight intron retention as an actionable vulnerability in advanced prostate cancer. *J Exp Clin Cancer Res.* 2024;43(1):58.
53. Shokry D, Khan MW, Powell C, Johnson S, Rennels BC, Boyd RI, et al. Refractory testicular germ cell tumors are highly sensitive to the targeting of polycomb pathway demethylases KDM6A and KDM6B. *Cell Commun Signal.* 2024 Oct 31; 22(1):528.
54. Lee H, Patschull AOM, Bagnérís C, Ryan H, Sanderson CM, Ebrahimi B, et al. KSHV SOX mediated host shutoff: the molecular mechanism underlying mRNA transcript processing. *Nucleic Acids Res.* 2017 May 5;45(8):4756–67. <https://doi.org/10.1093/nar/gkw1340> PMID: [28132029](https://pubmed.ncbi.nlm.nih.gov/28132029/)
55. Glaunsinger B, Ganem D. Lytic KSHV infection inhibits host gene expression by accelerating global mRNA turnover. *Mol Cell.* 2004;13(5):713–23. [https://doi.org/10.1016/s1097-2765\(04\)00091-7](https://doi.org/10.1016/s1097-2765(04)00091-7) PMID: [15023341](https://pubmed.ncbi.nlm.nih.gov/15023341/)
56. Glaunsinger B, Ganem D. Highly Selective Escape from KSHV-mediated Host mRNA Shutoff and Its Implications for Viral Pathogenesis. *J Exp Med.* 2004 Aug 2;200(3):391–8.
57. Clyde K, Glaunsinger BA. Deep sequencing reveals direct targets of gammaherpesvirus-induced mRNA decay and suggests that multiple mechanisms govern cellular transcript escape. *PLoS One.* 2011;6(5):e19655.

58. Ahlskog JK, Björk JK, Elsing AN, Aspelin C, Kallio M, Roos-Mattjus P, et al. Anaphase-promoting complex/cyclosome participates in the acute response to protein-damaging stress. *Mol Cell Biol*. 2010;30(24):5608–20.
59. Elsing AN, Aspelin C, Björk JK, Bergman HA, Himanen SV, Kallio MJ, et al. Expression of HSF2 decreases in mitosis to enable stress-inducible transcription and cell survival. *J Cell Biol*. 2014;206(6):735–49.
60. Yu Y, Wang SE, Hayward GS. The KSHV immediate-early transcription factor RTA encodes ubiquitin E3 ligase activity that targets IRF7 for proteasome-mediated degradation. *Immunity*. 2005;22(1):59–70. <https://doi.org/10.1016/j.immuni.2004.11.011> PMID: [15664159](https://pubmed.ncbi.nlm.nih.gov/15664159/)
61. Ren P, Niu D, Chang S, Yu L, Ren J, Ma Y, et al. RUNX3 inhibits KSHV lytic replication by binding to the viral genome and repressing transcription. *J Virol*. 2024;98(2):e0156723.
62. Gould F, Harrison SM, Hewitt EW, Whitehouse A. Kaposi's sarcoma-associated herpesvirus RTA promotes degradation of the Hey1 repressor protein through the ubiquitin proteasome pathway. *J Virol*. 2009;83(13):6727–38.
63. Broussard G, Ni G, Zhang Z, Li Q, Cano P, Dittmer DP, et al. Barrier-to-autointegration factor 1 promotes gammaherpesvirus reactivation from latency. *Nat Commun*. 2023 Feb 6;14(1):434.
64. Biswas A, Zhou D, Fiches GN, Wu Z, Liu X, Ma Q, et al. Inhibition of polo-like kinase 1 (PLK1) facilitates reactivation of gamma-herpesviruses and their elimination. *PLOS Pathog*. 2021;17(7):e1009764.
65. Zhang H, Wong JP, Ni G, Cano P, Dittmer DP, Damania B. Mitochondrial protein, TBRG4, modulates KSHV and EBV reactivation from latency. *PLOS Pathog*. 2022 Nov 23;18(11):e1010990.
66. Marquitz AR, Mathur A, Shair KHY, Raab-Traub N. Infection of Epstein–Barr virus in a gastric carcinoma cell line induces anchorage independence and global changes in gene expression. *Proc Natl Acad Sci*. 2012 Jun 12;109(24):9593–8.
67. Shannon-Lowe C, Rowe M. Epstein-barr virus infection of polarized epithelial cells via the basolateral surface by memory B cell-mediated transfer infection. *PLoS Pathog*. 2011 May 5;7(5):e1001338.
68. Temple RM, Zhu J, Budgeon L, Christensen ND, Meyers C, Sample CE. Efficient replication of Epstein-Barr virus in stratified epithelium in vitro. *Proc Natl Acad Sci U S A*. 2014;111(46):16544–9. <https://doi.org/10.1073/pnas.1400818111> PMID: [25313069](https://pubmed.ncbi.nlm.nih.gov/25313069/)
69. Corso S, Isella C, Bellomo SE, Apicella M, Durando S, Migliore C, et al. A Comprehensive PDX Gastric Cancer Collection Captures Cancer Cell–Intrinsic Transcriptional MSI Traits. *Cancer Res*. 2019;79(22):5884–96.
70. Molesworth SJ, Lake CM, Borza CM, Turk SM, Hutt-Fletcher LM. Epstein-barr virus gH is essential for penetration of B cells but also plays a role in attachment of virus to epithelial cells. *J Virol*. 2000;74(14):6324–32.
71. Murata T. Regulation of Epstein-Barr virus reactivation from latency. *Microbiol Immunol*. 2014;58(6):307–17. <https://doi.org/10.1111/1348-0421.12155> PMID: [24786491](https://pubmed.ncbi.nlm.nih.gov/24786491/)
72. Gomez-Pastor R, Burchfiel ET, Thiele DJ. Regulation of heat shock transcription factors and their roles in physiology and disease. *Nat Rev Mol Cell Biol*. 2018 Jan;19(1):4–19.
73. Lesch BJ, Page DC. Poised chromatin in the mammalian germ line. *Development*. 2014;141(19):3619–26. <https://doi.org/10.1242/dev.113027> PMID: [25249456](https://pubmed.ncbi.nlm.nih.gov/25249456/)
74. Sin H-S, Kartashov AV, Hasegawa K, Barski A, Namekawa SH. Poised chromatin and bivalent domains facilitate the mitosis-to-meiosis transition in the male germline. *BMC Biol*. 2015;13(1):53. <https://doi.org/10.1186/s12915-015-0159-8> PMID: [26198001](https://pubmed.ncbi.nlm.nih.gov/26198001/)
75. Wilkerson DC, Skaggs HS, Sarge KD. HSF2 binds to the Hsp90, Hsp27, and c-Fos promoters constitutively and modulates their expression. *Cell Stress Chaperones*. 2007;12(3):283–90. <https://doi.org/10.1379/csc-250.1> PMID: [17915561](https://pubmed.ncbi.nlm.nih.gov/17915561/)
76. Kallio M Brain abnormalities, defective meiotic chromosome synapsis and female subfertility in HSF2 null mice. *EMBO J*. 2002;21(11):2591–601.
77. Wang G, Zhang J, Moskophidis D, Mivechi NF. Targeted disruption of the heat shock transcription factor (hsf)-2 gene results in increased embryonic lethality, neuronal defects, and reduced spermatogenesis. *Genesis*. 2003;36(1):48–61. <https://doi.org/10.1002/gene.10200> PMID: [12748967](https://pubmed.ncbi.nlm.nih.gov/12748967/)
78. Joutsen J, Pessa JC, Jokelainen O, Sironen R, Hartikainen JM, Sistonen L. Comprehensive analysis of human tissues reveals unique expression and localization patterns of HSF1 and HSF2. *Cell Stress Chaperones*. 2024 Apr;29(2):235–71.
79. Sarge KD, Park-Sarge OK, Kirby JD, Mayo KE, Morimoto RI. Expression of heat shock factor 2 in mouse testis: potential role as a regulator of heat-shock protein gene expression during spermatogenesis. *Biol Reprod*. 1994;50(6):1334–43. <https://doi.org/10.1095/biolreprod50.6.1334> PMID: [8080921](https://pubmed.ncbi.nlm.nih.gov/8080921/)
80. Xing H, Wilkerson DC, Mayhew CN, Lubert EJ, Skaggs HS, Goodson ML, et al. Mechanism of hsp70i Gene Bookmarking. *Science*. 2005;307(5708):421–3.
81. Fehr AR, Yu D. Control the host cell cycle: viral regulation of the anaphase-promoting complex. *J Virol*. 2013;87(16):8818–25.
82. Elbasani E, Gramolelli S, Günther T, Gabaev I, Grundhoff A, Ojala PM. Kaposi's Sarcoma-Associated Herpesvirus Lytic Replication Is Independent of Anaphase-Promoting Complex Activity. *J Virol*. 2020;94(13):e02079-19.
83. Borozan I, Zapatka M, Frappier L, Ferretti V. Analysis of epstein-barr virus genomes and expression profiles in gastric adenocarcinoma. *J Virol*. 2018;92(2):e01239-17.
84. Hosseinipour MC, Sweet KM, Xiong J, Namarika D, Mwafongo A, Nyirenda M, et al. Viral Profiling Identifies Multiple Subtypes of Kaposi's Sarcoma. *mBio*. 2014;5(5):e01633-14.

85. Li X, Ohler ZW, Day A, Bassel L, Grosskopf A, Afsari B, et al. Mapping herpesvirus-driven impacts on the cellular milieu and transcriptional profile of Kaposi sarcoma in patient-derived mouse models. *bioRxiv*. 2024:2024.09.27.615429. <http://biorxiv.org/lookup/doi/10.1101/2024.09.27.615429> PMID: [39386738](https://pubmed.ncbi.nlm.nih.gov/39386738/)
86. Abere B, Samarina N, Gramolelli S, Rückert J, Gerold G, Pich A, et al. Kaposi's sarcoma-associated herpesvirus nonstructural membrane protein pK15 recruits the class II phosphatidylinositol 3-kinase PI3K-C2 $\alpha$  to activate productive viral replication. *J Virol*. 2018;92(17):e00544-18.
87. Ramaswami R, Tagawa T, Mahesh G, Serquina A, Koparde V, Lurain K, et al. Transcriptional landscape of Kaposi sarcoma tumors identifies unique immunologic signatures and key determinants of angiogenesis. *J Transl Med*. 2023;21(1):653. <https://doi.org/10.1186/s12967-023-04517-5> PMID: [37740179](https://pubmed.ncbi.nlm.nih.gov/37740179/)
88. Granato M, Romeo MA, Tiano MS, Santarelli R, Gonnella R, Gilardini Montani MS, et al. Bortezomib promotes KHSV and EBV lytic cycle by activating JNK and autophagy. *Sci Rep*. 2017;7(1):13052.
89. Shirley CM, Chen J, Shamay M, Li H, Zahnow CA, Hayward SD, et al. Bortezomib induction of C/EBP $\beta$  mediates Epstein-Barr virus lytic activation in Burkitt lymphoma. *Blood*. 2011 Jun 9;117(23):6297–303.
90. Joutsen J, Da Silva AJ, Luoto JC, Budzynski MA, Nylund AS, De Thonel A, et al. Heat shock factor 2 protects against proteotoxicity by maintaining cell-cell adhesion. *Cell Rep*. 2020 Jan;30(2):583–97.e6.
91. Elbasani E, Falasco F, Gramolelli S, Nurminen V, Günther T, Weltner J, et al. Kaposi's sarcoma-associated herpesvirus reactivation by targeting of a dCas9-Based transcription activator to the ORF50 promoter. *Viruses*. 2020 Aug 27;12(9):952. <https://doi.org/10.3390/v12090952> PMID: [32867368](https://pubmed.ncbi.nlm.nih.gov/32867368/)